AD NUMBER

AD455751

NEW LIMITATION CHANGE

TO

Approved for public release, distribution unlimited

FROM

Distribution authorized to U.S. Gov't. agencies and their contractors; Administrative/Operational Use; SEP 1964. Other requests shall be referred to Army Electronics Laboratories, Fort Monmouth, NJ.

AUTHORITY

USAEC ltr, 14 Oct 1969

DEFENSE DOCUMENTATION CENTER

FOR

SCIENTIFIC AND TECHNICAL INFORMATION

CAMERON STATION ALEXANDRIA, VIRGINIA

PT-825

Spencer Laboratory

Engineering Report
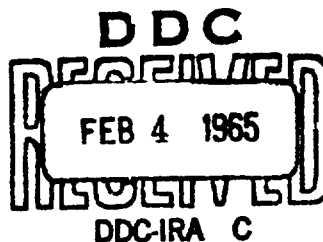
FINAL ENGINEERING REPORT

TWO STAGE X-BAND AMPLIFIER
FOR
HIGH RESOLUTION RADAR

Contract No. DA36-039-AMC-03202(E)
Department of the Army
Project No. 1P6-22001-A-055-04

July 15, 1963 - September 30, 1964

DDC

RECEIVED
FEB 4 1965

DDC-IRA C

U. S. Army Electronics Laboratories
Fort Monmouth, N. J.

RAYTHEON   RAYTHEON   COMPANY

MICROWAVE AND POWER TUBE DIVISION

DDC AVAILABILITY NOTICE

RAYTHEON COMPANY
Microwave and Power Tube Division
Spencer Laboratory
Burlington, Massachusetts

FINAL ENGINEERING REPORT

TWO STAGE X-BAND AMPLIFIER
FOR
HIGH RESOLUTION RADAR

Contract No. DA36-039-AMC-03202(E)

Electronics Command Technical Requirements
No. SCL-7001/88A, dated 25 March 1963

Department of the Army
Project No. 1P6-22001-A-055-04

July 15, 1963 - September 30, 1964

This report was written by W. Smith and edited by G. Saeger

This report has been approved by:

_____
J. F. Skowron, Manager,
Crossed-Field Amplifier Group

_____
L. Clampitt, Manager of Engineering,
Microwave Tube Operation

TABLE OF CONTENTS

TABLES

List of Illustrations

List of Illustrations (continued)

1 0   PURPOSE

1. 1   The propose of this project was to design, develop and deliver three X-band high-power amplifier chains for use in an airborne, high resolution radar.   Each chain, comprised of two Amplitron crossed-field amplifiers (QKS1243/QKS1244) and a ferrite isolator, produces a peak power output of 500 kilowatts at a gain of 27 db. The chains comply with the technical requirements set forth in SCL-7001/88A (amended).

1. 2   The QKS1243/1244 development program was begun 15 July 1963 and was completed on 30 September, 1964.

2.0   ABSTRACT

2.1 The QKS1243/1244 amplifier chain, developed and delivered by
Raytheon Company for a high resolution radar, is shown in Figure 1. Operating
at a band center frequency of 9500 Mc, its output stage, the QKS1243 Amplitron,
operates in either of two modes. In one mode, it produces a power output of
500 kilowatts at 0.0014 duty cycle and, in the other, it yields 250 kilowatts at
0.0028 duty cycle. The tubes are cathode pulsed and operate at a nominal efficiency
near 50%.

2.2   In developing the Amplitron tubes, some earlier experience was
used, but most facets of the tube designs were new.   During the program
engineering efforts were expended in developing new slow wave networks, a new
rf window, suitable air cooling fin geometries and in over-all ruggedization of the
tube to meet the vibration conditions.

2.3 The chain test program included, as design tests, a 300 hour life
test and operational vibration tests. For the former, 150 hours of operation at
the 500 kilowatt operating point was followed by 150 hours at the 250 kilowatt
(higher duty cycle) level.   The life test was accomplished without change of the
chain characteristics except for a slight power droop during the first fifty hours.
Vibration testing to MIL-E-5400 Specifications was performed with a chain operating
under full power conditions and was witnessed by the U.S. Army representatives.

2 4   Complete electrical acceptance tests were performed for, and
witnessed by, the U.S. Army on all three chains delivered.   These tests included
power output and phase versus frequency, efficiency and phase sensitivity to varia-
tions of pulse current.   Each of the three chains was demonstrated to be in full
compliance with the specifications.   That the gain, bandwidth, power output and
efficiency requirements were satisfied is shown by Figures 2 through 4, per-
formance curves for each of the chains.
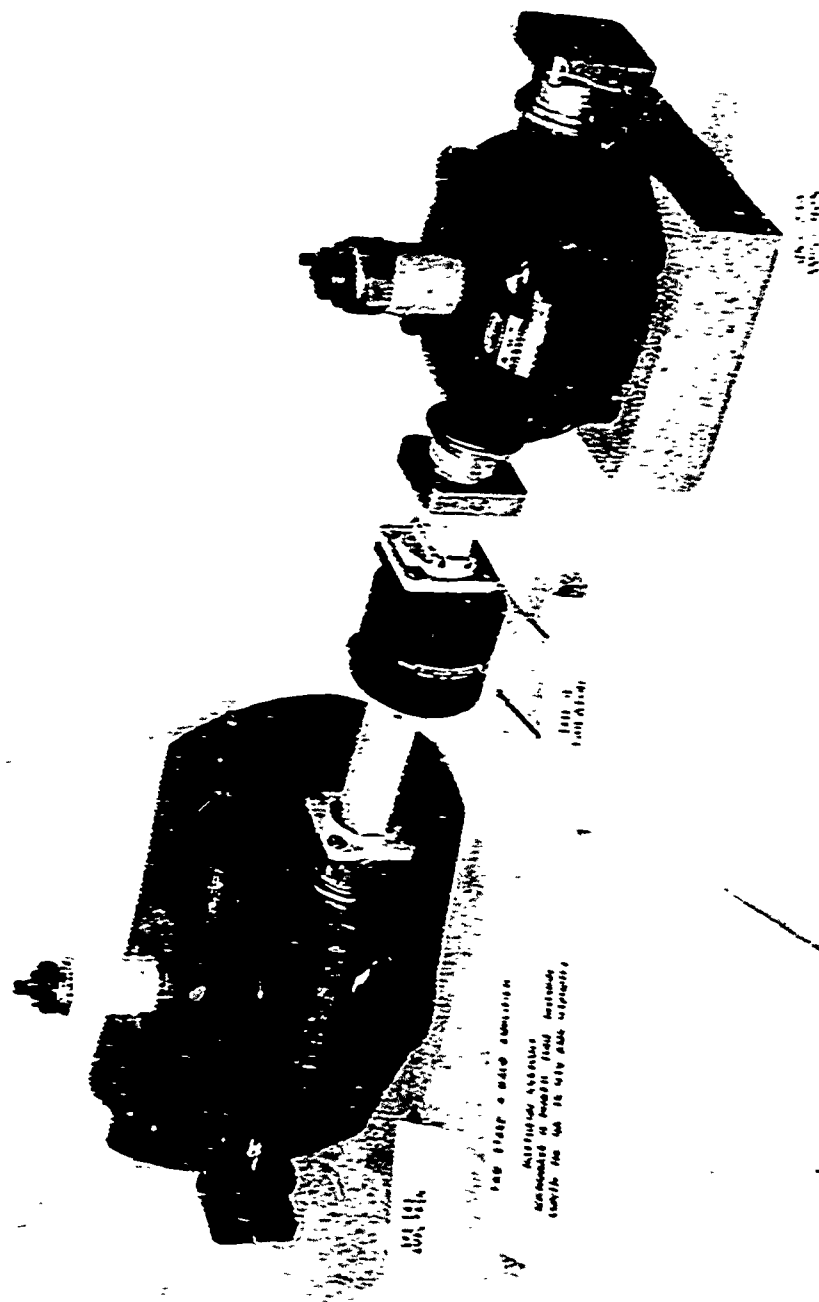
Figure 1 The QKS1243/1244 Amplifier Chain
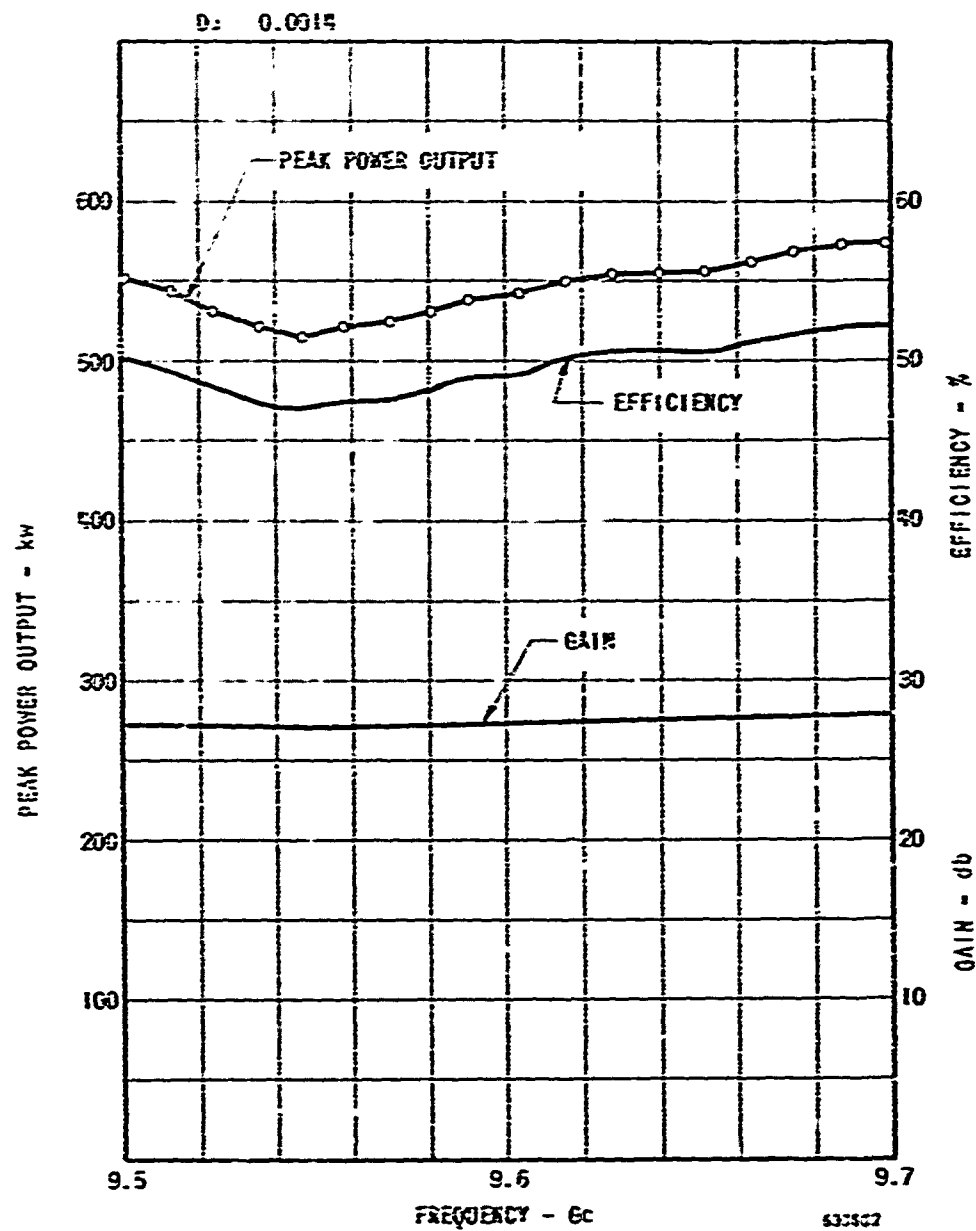
FIGURE 2   PERFORMANCE DATA QKS1243/1244   CHAIN #2

- 4 -
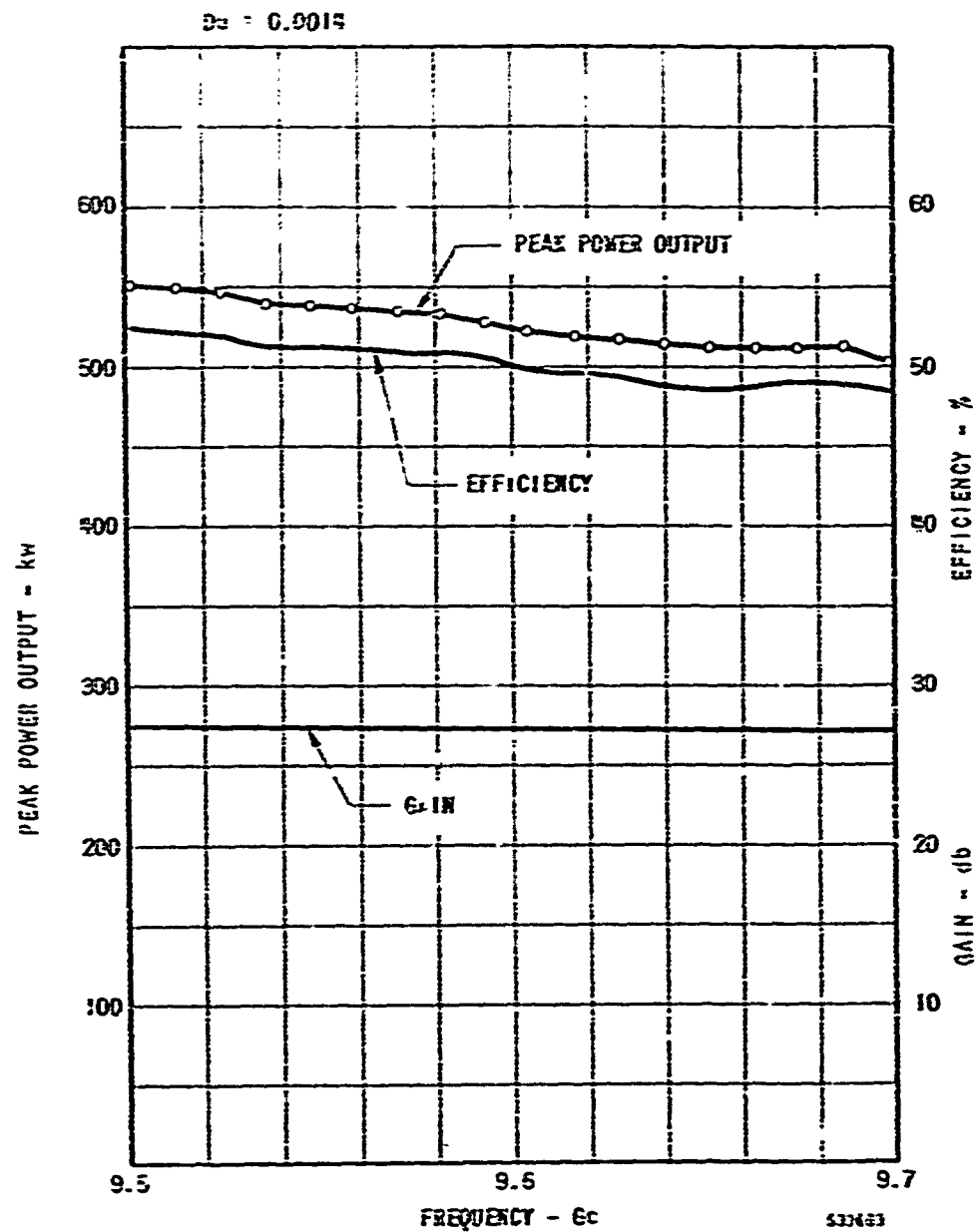
FIGURE 3   PERFORMANCE DATA QKS:243/1244 CHAIN #3

- 5 -
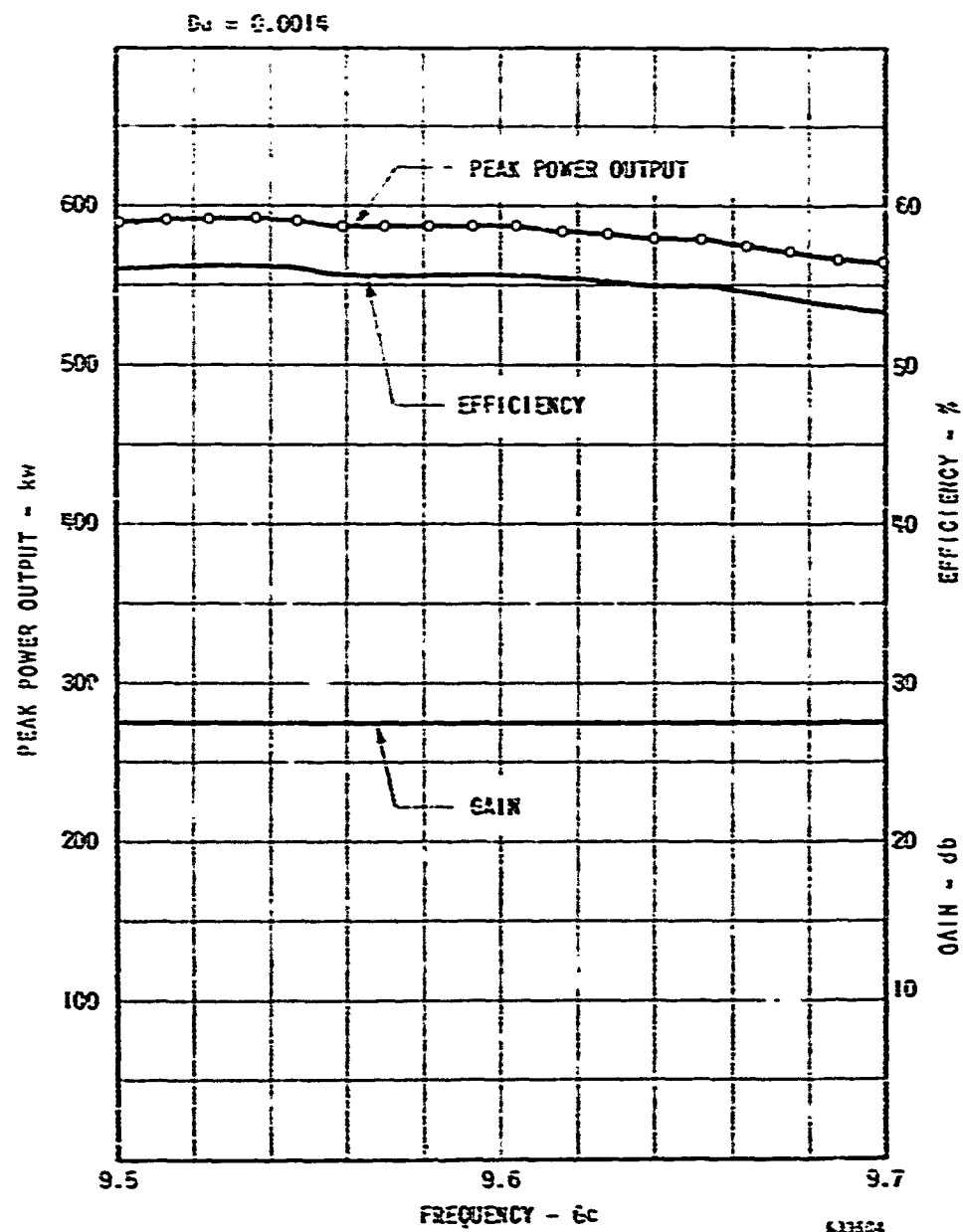
FIGURE 4   PERFORMANCE DATA QKS!243/1244 CHAIN #4

2.5   In the discussion and interpretation of the test results it is shown
that the measured phase sensitivities of the amplifier chains are better than those
which would be obtained from a TWT of equal gain.   This improvement is by a
factor of 2 with respect to voltage and a factor of 13 with respect to current.   It is
also shown that the linear component of power output (which is the predominant
component) has little effect upon system response.

2.6   In the concluding section recommendations are made which, when
implemented in additional chains, will result in more efficient and lighter
components.

PUBLICATIONS, LECTURES, REPORTS AND CONFERENCES

3 i   Progress reports to representatives of the U.S. Army Electronics
Laboratories were given on the following dates

Date	U.S. Army Participants	Raytheon Participants
25 July 1963	E. Kaiser	L. Clampitt, W. Smith
13 September 1963	N. Wilson	L. Clampitt, W. Smith, W. Stone
18 October 1963	N. Wilson	W. Smith
6 November 1963	N. Wilson	W. Smith
7 January 1964	E. Kaiser	W. Smith
2 February 1964	E. Kaiser	W. Smith
14 February 1964	E. Kaiser, K. Cunniff	W. Smith, R. Manchester
5 March 1964	E. Kaiser	W. Smith
15 April 1964	E. Kaiser	W. Smith
2 June 1964	E. Kaiser	W. Smith
9 June 1964	E. Kaiser, K. Cunniff	W. Smith, R. Manchester, W. Stone
26 June 1964	E. Kaiser	W. Smith, R. Manchester, W. Stone
20, 21 August 1964	E. Kaiser	W. Smith, R. Manchester, R. Andrews
16, 17 September 1964	E. Kaiser	W. Smith, R. Manchester, R. Andrews

4.0   GENERAL THEORY OF THE AMPLITRON

4.1 Amplitron tubes are characterized by a reentrant electron stream derived from a continuously emitting cylindrical cathode. The sheath of electrons, so formed, acting under the influence of a radial dc electric field and an axial magnetic field rotates about the cathode and interacts with fringing rf fields from a slow-wave network. The generalized slow-wave structure shown in Figure 5A could represent the interdigital structure common to the backward-wave oscillator, the loaded waveguide structure of a high power traveling-wave tube, or the vane structure of an Amplitron. These circuits are all similar in the sense that an electron beam passing adjacent to the circuit sees regions of rf field only between the circuit elements, while along the metallic element surface the tangential component of the rf field is zero. These circuits are also bandpass filters which will transmit only a particular band of frequencies bounded by radian cutoff frequencies ω_{c1} and ω_{c2}. At a specific frequency, the rf field distribution "seen" by the electron stream might be as shown in Figure 5 at a given instant of time. By the standard methods of Fourier analysis, such a waveform can be considered to be the sum of an infinite number of sinusoidal terms of form $E_m \sin \beta_m p$. Thus, every frequency has associated with it an infinity of terms (waves) of amplitude E_m and phase shift β_m radians/cell. A plot of the various β over all frequencies in the pass band of the circuit results in a most useful diagram called the $\omega-\beta$ diagram (see Figure 6).   The branch of this diagram from a to b represents all the fundamental terms of the Fourier series; the segment from b to c represents the second terms, etc. Branches other than the fundamental are termed space harmonics, and it is clear that the higher harmonics are weak in amplitude. Thus, we restrict ourselves to the fundamental and the first space harmonic for practical usage. For any circuit, in actual practice, one may obtain the $\omega-\beta$ diagram by a measurement of the phase shift per cell as a function of frequency. This yields all points on the fundamental branch. The space harmonic branches are then mirror images of the preceding branch so that they are also determined from the one measurement. A simple way of obtaining the data is to resonate a section of the circuit in a half wavelength mode. The phase shift per cell is then π radians divided by the number of cells in the circuit.
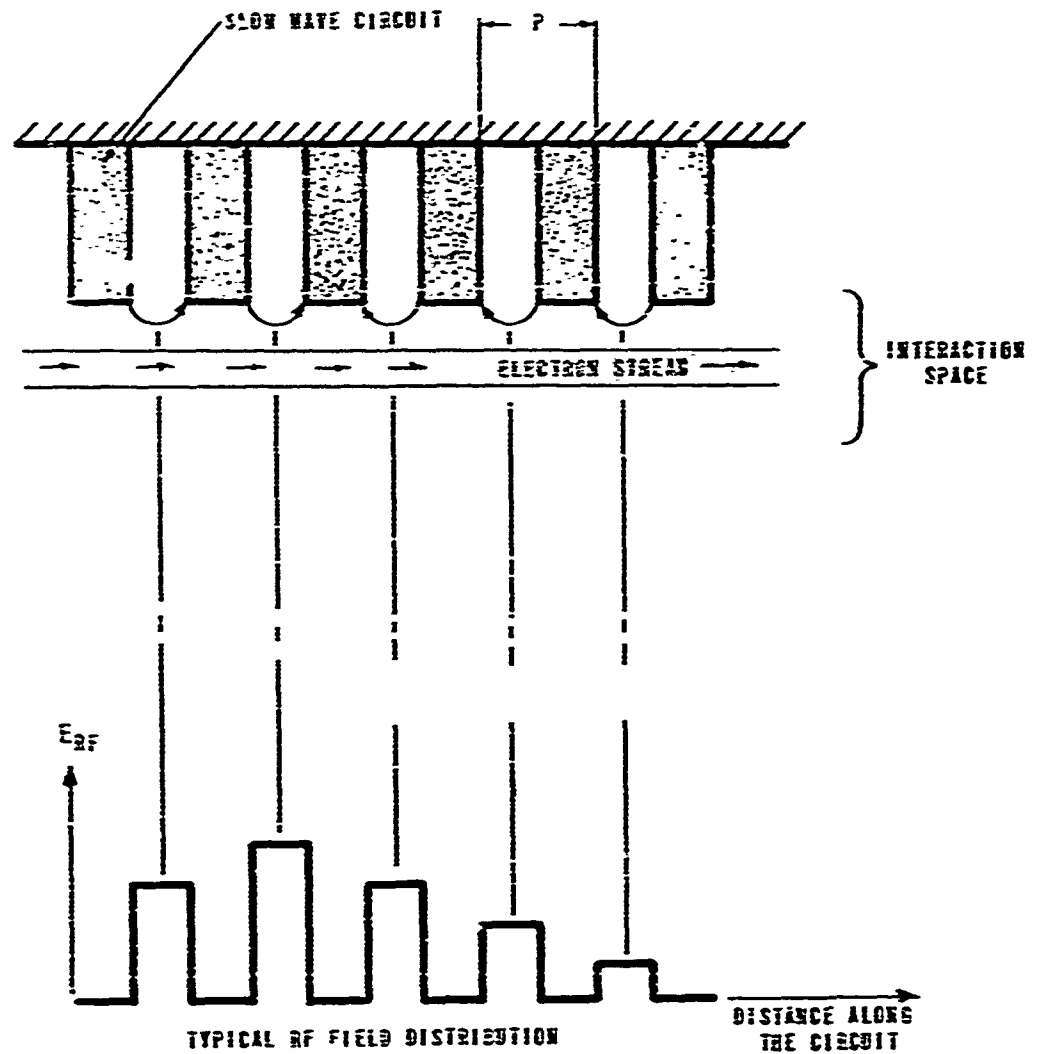
FIGURE 5   ELECTRON INTERACTION IN A CROSSED FIELD TUBE

627.437

- 10 -
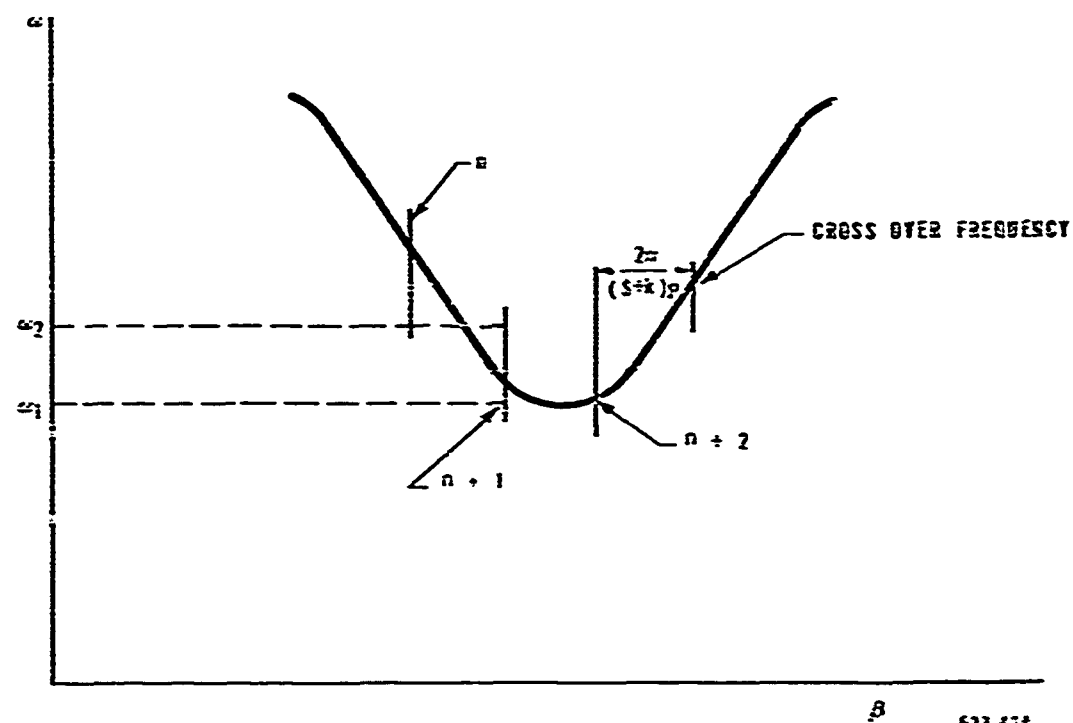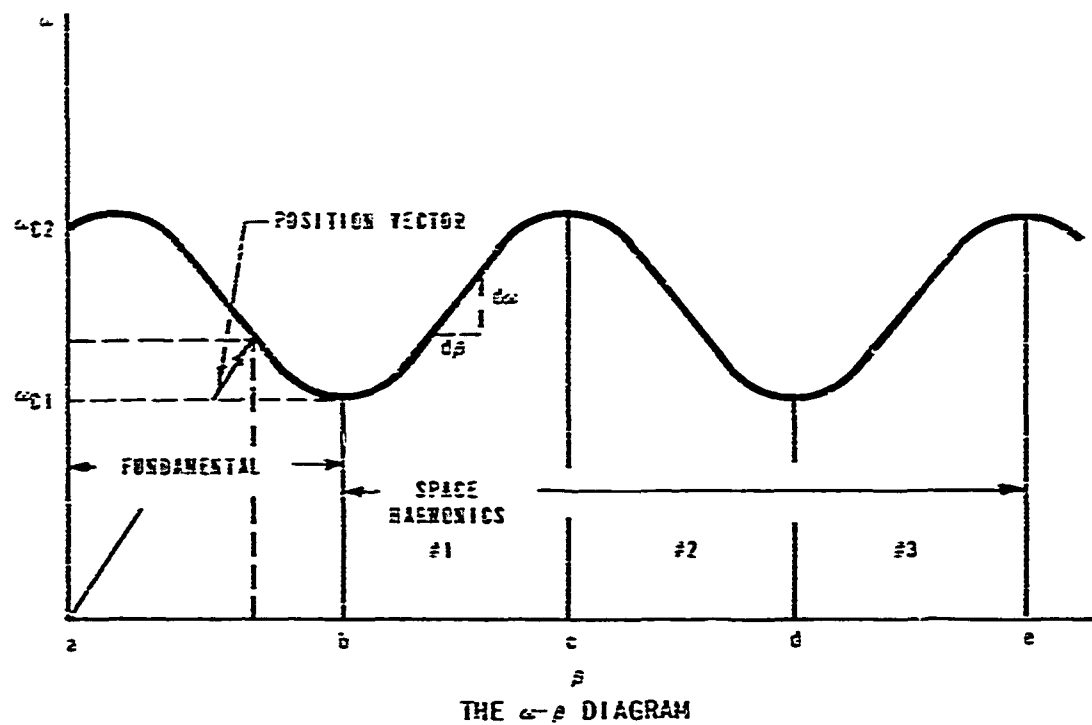
THE $\omega-\beta$ DIAGRAM

FIGURE 6   THE $\omega-\beta$ DIAGRAM FOR AN AMPLITRON

- 11 -

Having obtained the ω-β diagram, we make use of it by considering the slope of a position vector at any frequency of interest. This slope ω/β is, by definition, the velocity at which the wave appears to be traveling along the circuit to an observer in the interaction space. Thus, for example, the lowest fundamental phase velocity occurs at lower cutoff ω_{c1}, while at ω_{c2} the phase velocity goes to infinity. The space harmonic waves always travel more slowly.

The velocity of energy transport along the circuit is, by definition, $d\omega/d\beta$, i.e., the slope of the characteristic itself at any point. Notice that in the first harmonic branch the phase velocity and the energy (group) velocity are both positive while for the fundamental branch they have opposite signs. Physically, this means that to the electrons the fundamental waves appear to be traveling backwards with respect to the direction in which energy is actually flowing. The circuit represented by this diagram, therefore, is termed a backward-wave circuit. A backward-wave circuit always has a forward-wave space harmonic.

From our simple measurement, then, we have a result which tells us whether our circuit is forward-wave or backward-wave and what the phase and group velocities are on the circuit at any frequency in the pass band. What we would like to do next is to represent on the same diagram the various waves which can exist in the electron stream. Then we could see at a glance where amplification would take place since, for any microwave tube, the object of the game is to cause the beam waves and the circuit waves to propagate with equal, or near equal, velocities.

In the reentrant electron stream, many waves can exist. They have two basic requirements: (1) there must be an exciting force to set them up, and (2), since they always re-enter upon themselves, the sum of the phase shifts experienced during a single transit around the interaction space must be an integral multiple of 2π radians. The excitation force is derived from the rf voltages on the circuit so that the electron stream waves are strong only near a point where the beam characteristic crosses the circuit characteristic. Because of the reentrancy condition, the beam waves can occur only at phases

satisfying the requirement that the total phase shift in one transit be $2\pi n$ radi-
Thus, at a given frequency, waves are possible for which n = 1, 2, 3 ..... and
these can be represented by vertical (constant phase) lines on the ω-β diagram,
as shown by Figure 6B. The crossover phases will be determined from the
relation.

$$(S + k)\ \beta p = 2\pi n$$

where

S = the number of network cells in the circuit,

k = the length of the drift section between input and output.

p. = the length (pitch) of one section, and

n = any integer

By rewriting this relation in the form

$$\beta = \frac{2\pi n}{(S + k)\ p}$$

it may be seen that the more sections (S) are used in a given tube the smaller the
spacing between the vertical lines will be, or in other words, more space charge
waves will be possible over a given range of β values. These vertical lines, which
represent the waves on the electron stream, are called space-charge modes. The n
number of the space-charge mode corresponds to the number of spokes of space
charge. As for the circuit waves, the velocity of the space-charge wave is given
by the slope of the position vector. Since the velocity for a fixed magnetic field
is a function of the voltage, one may see at a glance the relative operating voltage
in the vicinity of any crossover point, the point of maximum interaction between
the circuit and the space-charge mode.

To amplify in the vicinity of any crossover frequency, rf drive at
that frequency must be supplied to excite the space-charge mode, and the proper
voltage must be applied to the tube to correspond to the velocity requirements of
that particular space-charge mode. Energy exchange then takes place. If the
frequency departs from the crossover frequency, it is obvious that the velocity

of the circuit wave beings to differ from that of the space-charge waves, making interaction more difficult, but, if the rf drive power is great enough, a wide band of frequencies can be amplified without losing control of the space charge. This is the Amplitron principle - interaction between a single space charge mode and the circuit. The band center frequency, of course, corresponds to the crossover frequency. Because of the re-entrancy requirements on the space-charge waves, it is seen that the velocity of the space charge waves, and thus the operating voltage of the tube, must vary directly with the applied frequency. This situation exists whether or not we are using a forward-wave circuit or a backward-wave circuit.

      4.2 Much useful design information can be derived from computations of characteristic voltage, magnetic field and power output. Relations for these follow:[1]

* Characteristic Voltage $V_o = 2.56 \times 10^5 \left(\frac{\pi d_a}{n\lambda}\right)^2 (2.54)^2$ (1)

* Characteristic Magnetic Field $B_o = \dfrac{21200}{n\lambda \left[1-\left(\frac{dc}{da}\right)^2\right]}$ (2)

* Characteristic Power $P_o = \dfrac{43.6 \times 10^8 \, (0.9) \, h}{\left[1-\left(\frac{dc}{da}\right)^2\right]^2 \left[1+\left(\frac{da}{dc}\right)\right] da} \left(\frac{\pi d_a}{n\lambda}\right)^5 (2.54)^5$

     (3)

where d_a = anode diameter in inches,

       n = the space charge mode number,

       λ = the operating wavelength in centimeters,

       d_c = the cathode diameter in inches, and

       h = the active anode length in inches.

---

1 Derivations of Vo, Po, and Bo can be found in Collins, Microwave Magnetrons, McGraw-Hill, 1948, p. 416.

4.3 The operating voltage, in terms of operating magnetic field, is given by equation 4.

$$\frac{V}{V_o} = 2 \frac{B}{B_o} - 1 \qquad (4)$$

4.4 It can be shown that the efficiency obtainable from a given crossed-field tube is intimately related to the ratio B/B_o. Hence, one can select a B/B_o ratio corresponding to the desired efficiency as a starting point for the design. Then, through the specified voltage and equation 4, other parameters can be chosen. A guide to the relation between B/B_o and efficiency is given by the empirical curve of Figure 7.

4.5 Bandwidth capabilities are indicated by reference to Figure 6. If one departs from the band center (crossover frequency) in either direction, eventually there will be sufficient velocity slip between the space-charge waves and the circuit waves to shift interaction from the desired space-charge mode to an adjacent mode. The transition will be accompanied by voltage and current discontinuities and, therefore, must be avoided by restriction to the design mode. If the number of sections $(S \div k)$ is small, bandwidth capability will be increased since the β separation of the space-charge modes will increase. For a given value of $(S \div k)$, greater circuit bandwidth will lead to greater operating bandwidth because of the consequent reduction of the absolute velocity slip at a given frequency. By combinations of these methods, up to 25% bandwidth has been obtained in practice. The technique must be used with caution, however, since increases of bandwidth are necessarily coupled with reductions of gain capability for a given type of slow-wave network.

4.6 Examination of the characteristics of a large number of differing Amplitron types leads to the approximation that about 10 db of gain will be obtained at 3.5 Po (characteristic power) and that 17 to 18 db can be obtained near Po.

4.7 By judicious selection of the design parameters, we can reasonably well determine in advance the expected voltage, efficiency, power output, gain and bandwidth of a proposed tube.
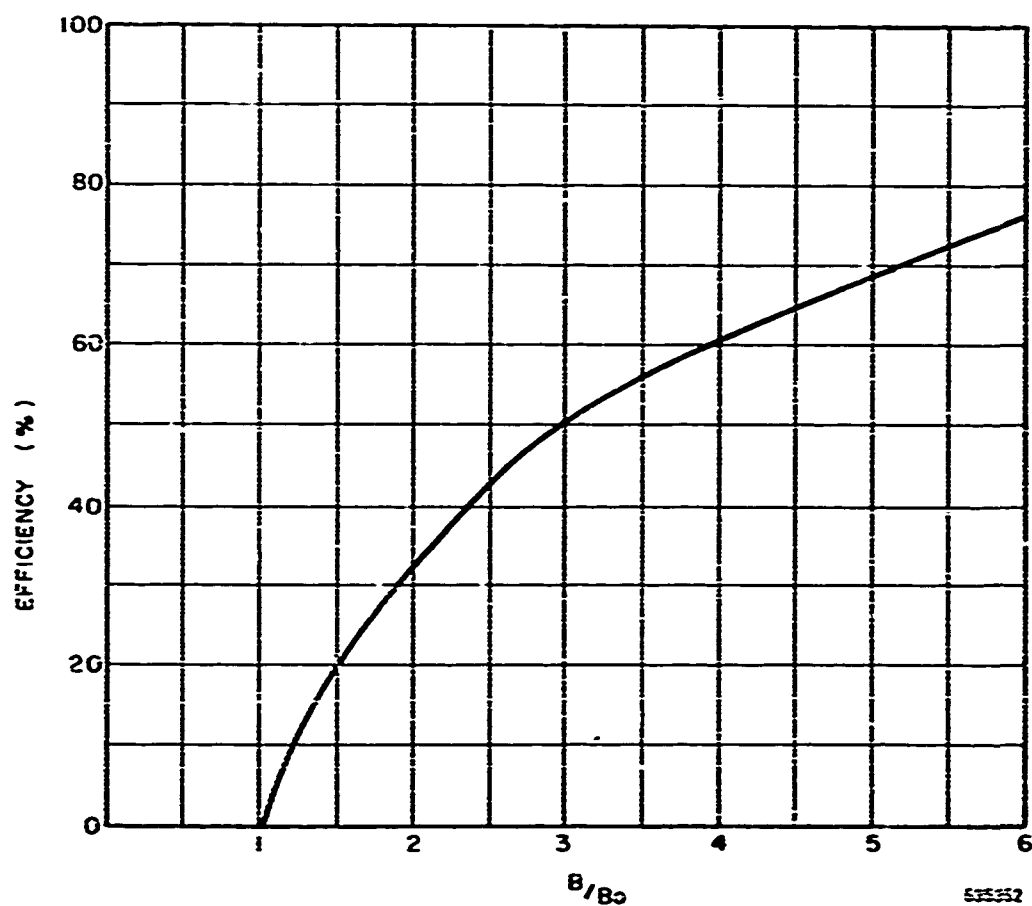
FIGURE 7   EFFICIENCY AS A FUNCTION OF B/B_0

(EMPIRICAL DATA)

- 16 -

5. 0   FACTUAL DATA

5. 1   General Information

5 1 1   The output stage of the two-stage amplifier, shown in Figure 8,
is designated as QKS1243.   The driver stage, designated the QKS1244, is shown
in Figure 9.   These two Amplitron tubes with a Raytheon IXH24 ferrite isolator
form the two-stage amplifier snown pictorially in Figure 1 and in block diagram
form in Figure 10.

5 1.2   When supplied with a 1 kilowatt (peak) rf input signal the amplifier
will produce an output power of 500 kilowatts at .0014 duty factor or 250 kilowatts
at .0028 duty factor.   The bandwidth is 150 Mc minimum, centered at 9600 Mc,
but greater bandwidth capability is available from the design.   Both stages employ
integral permanent magnets, are cathode-pulsed and use forced air cooling.   The
waveguide input and output on each tube is furnished in RG-51/U waveguide
(5/8" x 1-1/4") and the waveguide flanges mate with cover flange type UG-51/U.

5.1 3   The two-stage amplifier has been designed to operate at altitudes
of 40,000 feet under the temperature conditions specified for Class 1 equipment in
MIL-E-5400.   The high voltage bushings require pressurization.   The tube chain
has been tested under operating conditions to the vibration requirements of
MIL-E-5400.

5. 1. 4   Although the specified minimum over-all efficiency of the chain
is 40% the actual observed efficiencies are nominally 50%.   The weight of the
entire chain comprising two tubes plus isolator, is 45.6 lb.   A reduction of
approximately 5 lb is feasible.
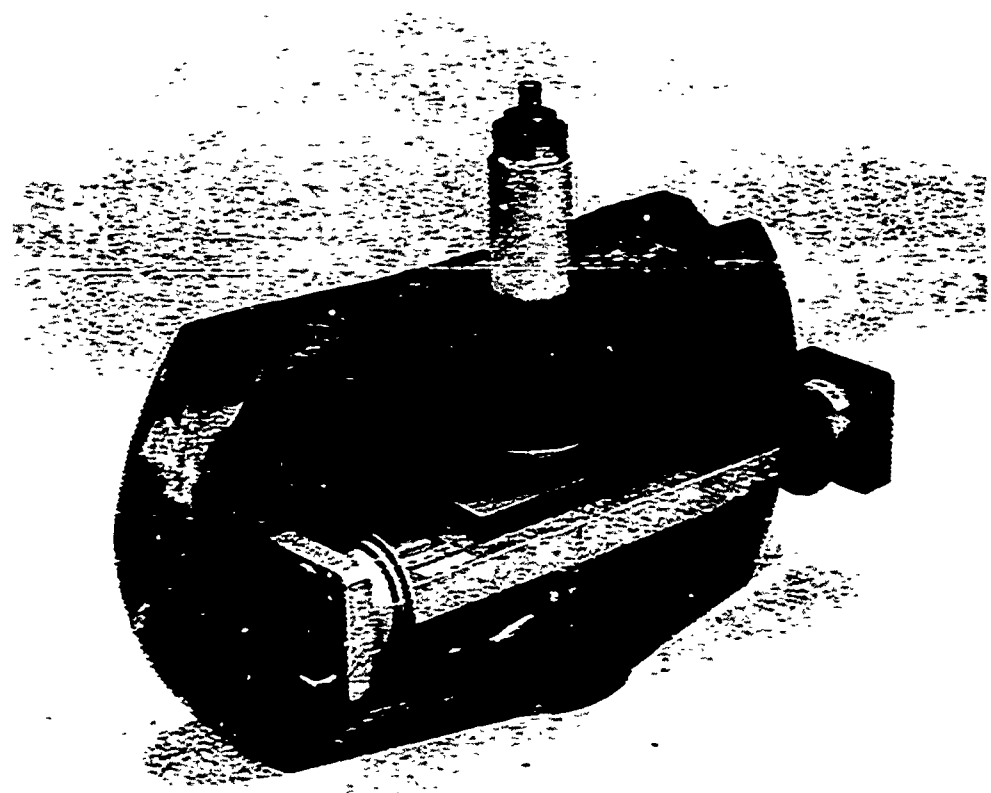
54 2-203

Figure 8   The QKS1243 Amplitron

- 15 -
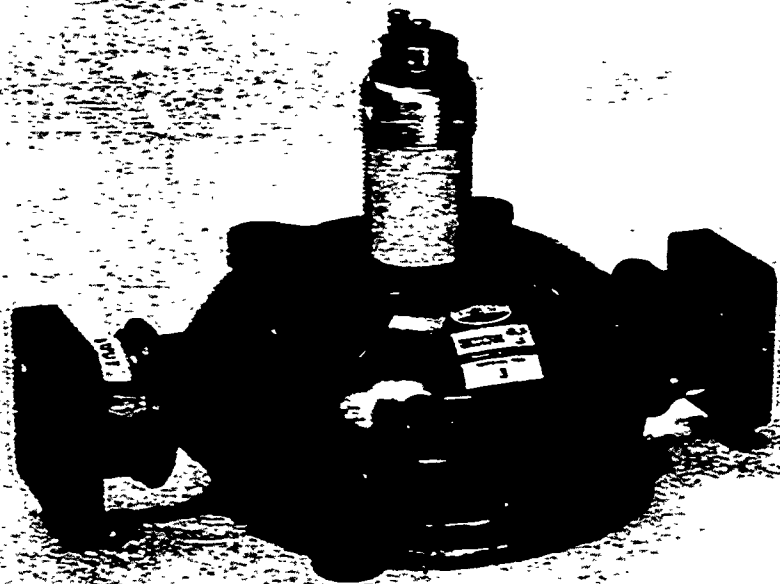
Figure 9 The QKS1244 Amplitron

RF INPUT — 1 KW / 1 KW → QKS1244 AMPLITRON 16 KV 0.6 POUNDS — 25 KW / 25 KW → IXN 24 ISOLATOR 2.1 POUNDS — QKS1243 AMPLITRON 30.6 KV 35.0 POUNDS — 500 KW / 250 KW → RF OUTPUT — OPERATION I / OPERATION II
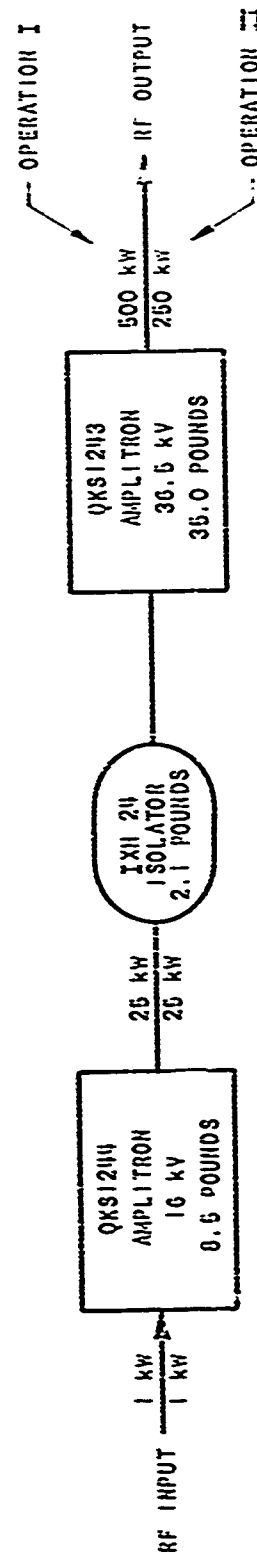
633580

BLOCK DIAGRAM - QKS1243/1244 AMPLIFIER CHAIN

FIGURE 10

5 1.5   For reference purposes the major electrical and mechanical specifications of SCL-700 1/88A, which the tube chains had to satisfy, are given below.

Electrical	Operation I	Operation II
Peak Power Output	500 kw (min)	250 kw (min)
Duty Cycle	0.0014	0.0028
Pulse Width	2.0 μs	2.0 μs
Efficiency	40% (min)	40% (min)
Center Frequency	9600 Mc	9600 Mc
Instantaneous Bandwidth	150 Mc (min)	150 Mc (min)
RF Drive	1 kw (max)	1 kw (max)
Phase Linearity . . .	The phase versus frequency characteristic will be taken as the summation of a linear component, a first-order sinusoidal component and higher order components. The first order component may be no greater than one-half cycle over the required frequency band, and its amplitude must be less than 26 degrees. Higher order components must have amplitudes less than 4.0 degrees. Stated mathematically, the requirement is	

$$B_{(\omega)} = b_0 \, \omega \div \sum_{n} \, b_n \sin n \, c \, \omega$$

where $B_{(\omega)}$ is the steady-state phase char-
acteristic

$$\omega = 2 \pi f$$

$$b_0 = \text{a constant}$$

$$b_1 \leqq 26^{\circ}$$

$$b_{n>1} \leqq 4.0^{\circ}$$

$$c \geqq \frac{1}{2 \times 150 \times 10^{6}}$$

Amplitude Flatness	< 0.5 db, and ± 0.3 db for components > 2 cycles
Phase Sensitivity	≦ 1.5 degrees per 1% variation of pulse power.

<u>Mechanical</u>

Temperature-Altitude	per MIL-E-5400. Class I
Cooling	forced air
Shock	per MIL-E-5400
Vibration	per MIL-E-5400. Class I

5.2   Development of the QKS1243

5.2.1   <u>Design Parameters</u>

5.2.1.1   The final parameters for the interaction space design of the QKS1243 are presented in Table I below.

<u>Table I</u>

<u>QKS1243 Design Parameters</u>

Band center frequency. fo	9600 Mc
Number of active network sections. S	18
Drift section length (in network pitches).k	2
Network pitch. p	0. 0772 in.
Space charge mode number. n	8
Anode diameter. da	0. 492 in.
Cathode diameter. dc	0 280 in.
Characteristic voltage. V_o	6310 volts
Characteristic magnetic field. Bo	1254 gauss
Characteristic power. Pc	371 kw
Approximate B/Bo ratio	3. 26
Operating voltage	36. 5 kV
Interaction space length. n	0. 616 in.

5.2.2   <u>The Phase Frequency Characteristic of the Slow-Wave Circuit</u>

5.2.2.1   The proper phase frequency characteristic for the QKS1243 was determined through comparison of the hot and cold test results of several tubes. A final design. represented by cluster[2] #20 which was used in tube #F (chain #3) is documented by Figures 11 and 12.   Figure 11 shows a resonance plot obtained by

---

2.   A cluster is an slow wave circuit assembly comprised of vanes straps and end covers

FREQUENCY - Oc

PERCENT REFLECTION - REFLECTOMETER

100

75

50

25

8129 KC

8725 KC

9125 KC

9560 KC

10079 KC
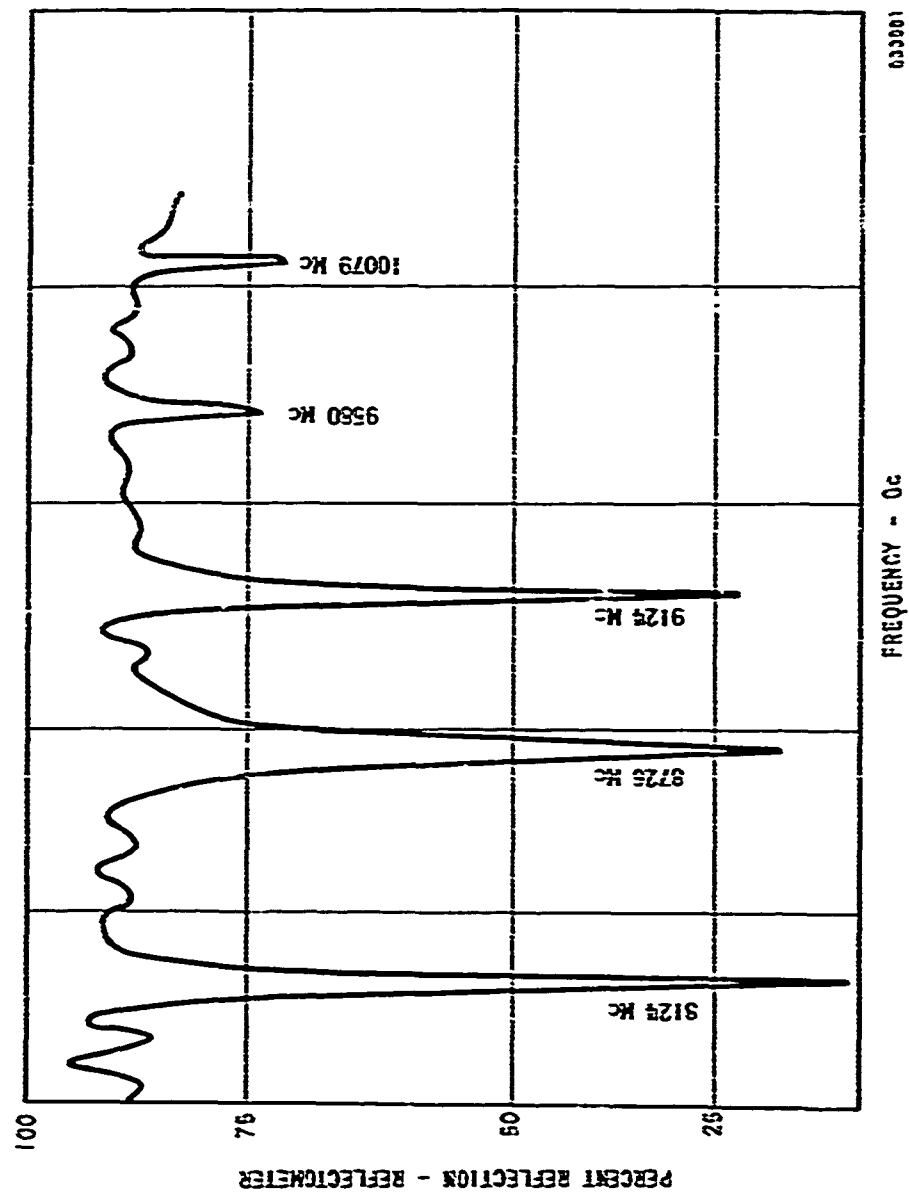
RESONANCE PLOT QKS12113 (CLUSTER #20)
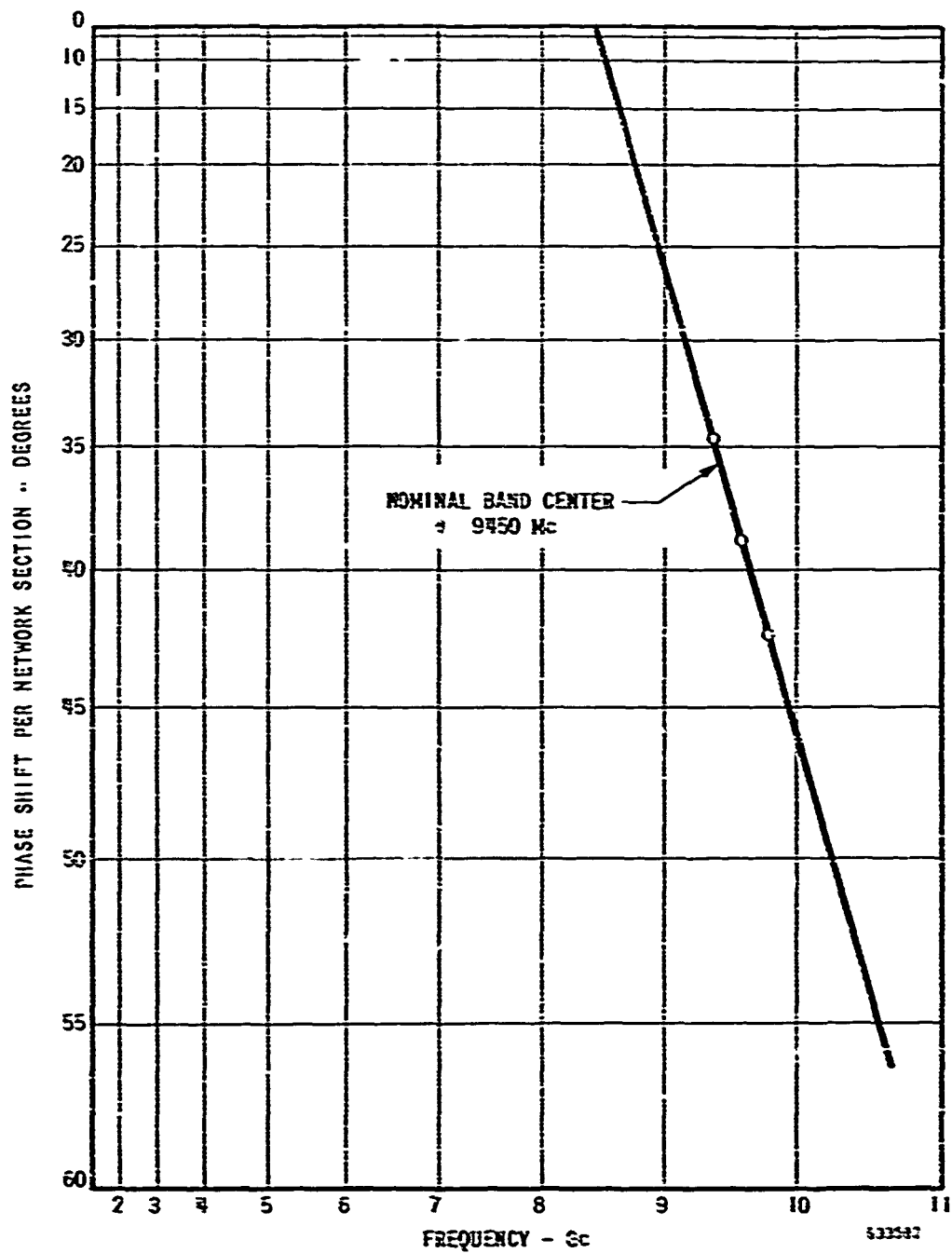
FIGURE II

FIGURE 12   QKS1243 CLUSTER #20 PHASE DATA

- 24 -

terminating the waveguide of a standard reflectometer with a cylinder containing the cluster assembly. The cluster assembly is inserted with the free, or floating, strap closest to the mouth of the waveguide and with the drift space adjacent to one of the narrow walls of the waveguide. The plot is useful as a control for electrically duplicating a satisfactory assemble. Figure 12 shows the phase shift per section versus frequency characteristic obtained by measurement of standing waves on the slow wave network. This method gives true phase shift but is time consuming. When correlation between the two methods is obtained by examination of hot test performance data, the resonance plot method is more accurate for additional assemblies.

5.2.3   Network Matching

5.2.3.1   Matching of the slow wave structure to the uniform waveguides was accomplished in the usual fashion using ramps and two-wire transmission lines. Data representative of the final design (obtained from QKS1243 #G-Chain #4) are shown in Figure 13. These data show the input reflection coefficient when the output of the Amplitron is terminated by a matched load and therefore include the lumped effects of the input and output transducer mismatches

5.2.4   Spectral Power Distribution

5.2.4.1   In addition to achieving the best possible match over the desired operating band to secure good phase-frequency linearity, it is also desirable to match the impedance of the slow wave network all the way to the lower cutoff frequency. This requirement can conflict with obtaining an optimum match in the required band. If the match could be made ideal, i.e., network matched everywhere, the Amplitron would produce essentially no spurious power. This is because most Amplitron spurious signals are generated during the rise and fall times of the modulating pulse when the space charge is synchronous with the lower frequency circuit waves. In practice, however, an ideal match cannot be attained, although in some Amplitron types it has been approached. In the case of the QKS1243 and QKS1244 the best possible match was obtained within the given time and funding, primarily concentrating on the in-band match. The results were adequate, as determined by measurement of the spectral signature of a complete chain. These data are shown in Figure 14. It is expected that in additional tubes the spectral level can be reduced to -35 db in all regions and to -40 db in most

- 25 -
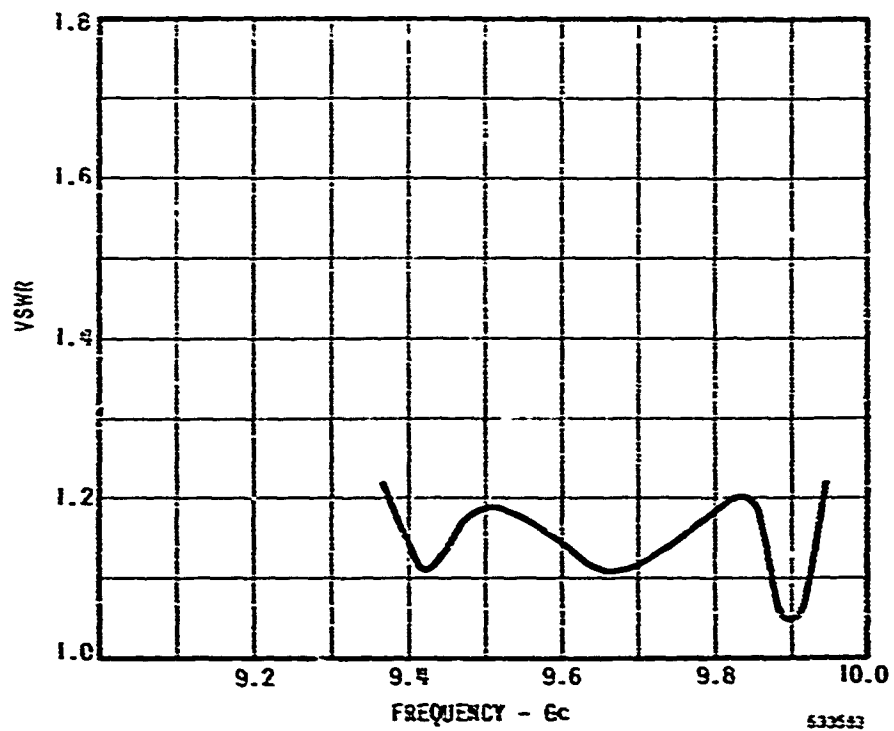
FIGURE 13   INPUT VSWR vs FREQUENCY
                        QXS1243 #4
                   (MATCHED TERMINATION)

- 25 -
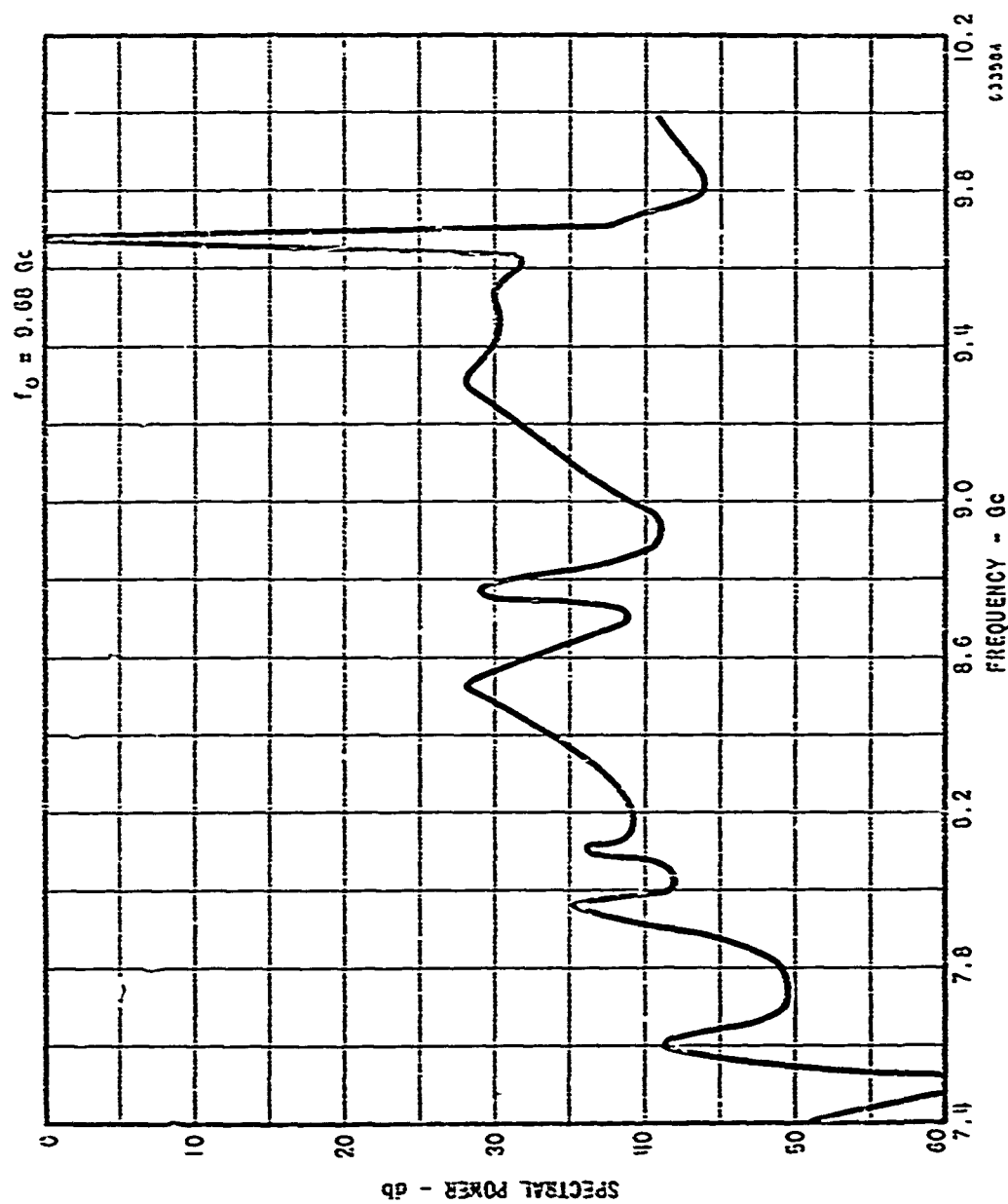
SPECTRAL POWER DISTRIBUTION
QKS1243/1244 CHAIN #4

FIGURE 14

5.2.5 RF Windows

5.2.5.1 An improved rf window design was developed specifically for the QKS1243/1244 program. A pillbox design, the window is simple mechanically and easily fabricated. An rf match typical of the design is given in Figure ˙˙ Midway in the program, it was found that welding the window to the tube body sometimes resulted in frequency regions of abnormally high insertion loss. Consequently, the windows of all tubes shipped were brazed to the tube body

5.2.6 Cold Cathode Operation

5.2.6.1 Cold cathode operation of the QKS1243 was anticipated from the beginning and was, in all instances, completely successful and free from jitter. Therefore, these tubes were supplied with only a single binding post connection for the high voltage lead. To avoid any problems of long range sagging of the cantilever mounted cathode, vertical mounting of the tube's input bushing was recommended.

5.2.7 Cooling Analysis

5.2.7.1 The QKS1243 Amplitron was required to have a forced-air cooled anode, and had to meet the requirements of MIL-E-5400 for Class I equipment to an altitude of 40,000 feet. The cooling air temperature at that altitude is nominally $31^{\circ}C$ and intermittently up to $47^{\circ}C$. It was assumed that for satisfactory cooling, the hot spot on the external surface of the tube would have to be less than $125^{\circ}C$. The hot spot on the internal surface of the anode would have to less than $450^{\circ}C$ for the $31^{\circ}C$ ambient temperature.

5.2.7.2 The maximum anode dissipation was assumed to be 1050 watts (700 watts output at 40% efficiency). It was assumed that the hottest vane is located in the worst position for cooling (adjacent to the drift vane) and that its dissipation must be twice the average for all 20 vanes. It was further assumed that 80% of its dissipation is uniformly distributed over the center 0.35 inches of the vane face. For the fin design, it was assumed that dissipation in the general area of the worst vane would be 1.5 times the average.
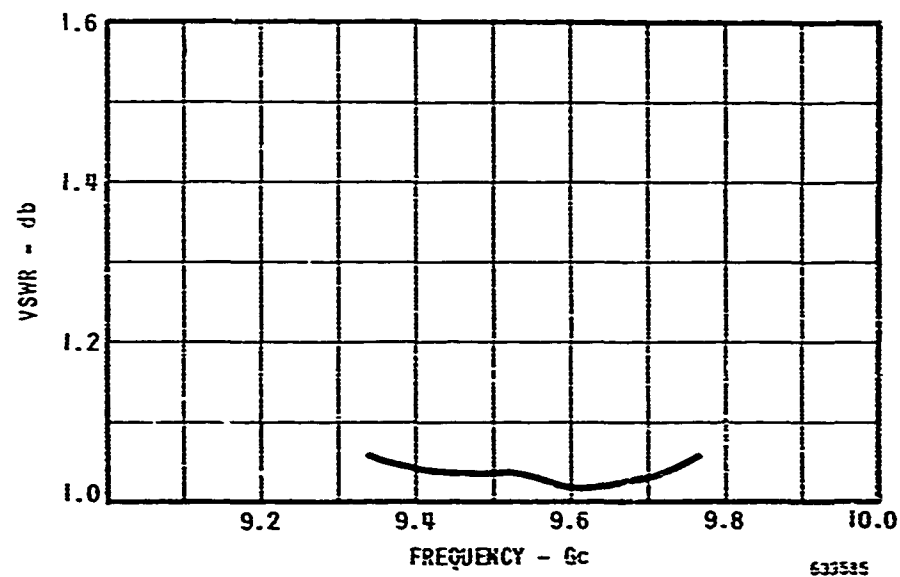
FIGURE 15   INPUT VSWR vs FREQUENCY
QKS1243/1244   RF WINDOW #25
(MATCHED TERMINATION)

5.2.7.3   The design which was analyzed and used in the tubes was defined by Raytheon drawings

B626933-1, A627470-2, A626862-0, A626883-0, A623443-1, A623444-1, A626939-1, B626940-4, B627121-2, B627122-2, B627123-2, A623434-3

This design shown in the outline drawing of Figure 16, is reasonably optimized but improvements could be made with additional effort.   The fin geometry with regard to thickness, spacing and size cannot be significantly improved. Reduction of the fin spacing would increase air flow resistance too much; reduction of the fin thickness would decrease fin effectiveness too much; increasing the fin size would also decrease fin effectiveness too much.   The use of interruption tabs in the air flow path would increase flow resistance, but might result in a net improvement in cooling with careful design.

5.2.7.4   A change that would aid cooling efficiency from two points of view would be to increase the number of fins from the present 23 to 27 by increasing the anode height.   With this change, it would also be desirable to increase the spacing between fins, since it is now difficult to prevent solder from bridging the fins.   Going to 27 from 24 fins, as an example, would reduce air flow requirements by 10% and pressure drop by 20%.

5.2.7.5   Computations of air flow and total anode pressure drop requirements were made.   The results are given in Table II for both sea-level and 40,000 feet, with the corresponding inlet air temperatures as given in MIL-E-5400.   Because the highest dissipation is assumed to be near the waveguide side of the anode, the results are different for the two possible air flow directions. The positive direction of air flow is defined as supplied from the rectangular fin entrance and exhausted at the waveguide end of the fins.

Figure 16   Outline Drawing QKS1243

OBJECTIVE
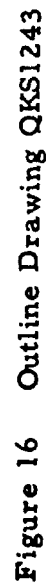
TABLE II

TABULATION OF COOLING ANALYSIS RESULTS

Air Flow Direction	Positive	Positive	Negative	Negative
Altitude feet	0	40,000	0	40,500
Inlet temperature $^{\circ}C$	55	31	55	31
Mass flow rate, lb/min.	5.0	3.0	3.8	2.3
Inlet density, lb/ft^3	0.067	0.0137	0.067	0.0137
Inlet flow rate, CFM	75	220	57	168
Anode pressure drop, inches of H_2O	1.6	5.0	1.1	3.8

5.2.7.6 It is assumed that air will be supplied at the above pressures and temperatures from a general air supply in the aircraft. The air blower must be placed downstream to pull air through the fins since the dissipation and temperature rise due to the blower will be too high to allow cooling air to be supplied from the blower. The negative air flow direction is most logical, both mechanically and thermally, for exhaust blower cooling. Filtering of the inlet air is recommended, if possible

5.2.7.7 The worst performance point for the blower (at nominal conditions) is at maximum altitude. With the above exhaust blower arrangement, the bulk temperature rise through the anode is $60^{\circ}C$ at altitude, and the blower must move 203 CFM of air (heated by the anode) at a density of 0.0113 lb/ft^3 against a head of 3.8 inches of H_2O. The blower inlet is $91^{\circ}C$, and the outlet may be as high as $150^{\circ}C$

5.2.7.8 At the intermittent condition of $47^{\circ}C$ inlet air temperature, a blower just meeting the above point will fall off about 5% in mass flow rate. The anode hot spot temperatures will be increased about $20^{\circ}C$, and the blower inlet temperatures will be about $111^{\circ}C$ and the outlet as high as $175^{\circ}C$.

5.2.7 9   The Globe VAX-4.5-LC Vaneaxial blower will suffice for the QKS1243 Amplitron. This unit is slightly under-sized for operation at 40% efficiency and at maximum altitude the anode temperature would be about 20°C hotter than with the design flow. Since the actual efficiency is 50% the recommended blower is entirely adequate.

5.2.7 10   Anode cooling in this design is of a nature described by fully developed laminar flow (limiting Nusselt number). As such, cooling with the above blower will greatly improve as altitude is reduced, as a result of high mass flow, even for a high-slip motor. This type of motor is desired for this application because it allows the blower speed to drop off as it is more heavily loaded at low altitude, reducing motor power consumption.

5.2.8   High Voltage Bushing Design

5.2.8.1   Because operation of the amplifier chain at a 40,000 foot altitude was a design requirement, voltage breakdown testing was begun early in the program. Using a bushing formerly used successfully in the QKS506 Amplitron[3], modifications were incorporated to render it less prone to breakdown at a given voltage. The results of tests on this bushing design are shown in Figure 14 with a more or less ideal curve[4] included for comparison. Indicated also is the operating gradient required if a bushing of the original length were to be used.

5.2.8.2   Some efforts were expended in testing trial geometries which might increase the breakdown potentials, notably the use of corona shields and rounded edges where possible. These efforts were not successful. The alternative was to increase the bushing length to provide the required operation with a reasonable safety factor. This, however, would require a bushing 6 inches in length, a length incompatible with the vibration requirements.

5.2.8.3   One alternative design investigated is shown in the X-ray photograph of Figure 18. Surrounding the bushing is a metallic shell filled with material of high dielectric strength. From the top of the shell a flying lead is brought out, and the shield of the flying lead is bonded to the shell. The grounded construction was used because in earlier potting experiments it was found that

---

3   DA36-039-SC-85331

4   From data in "Electronics", Millman and Seely, McGraw-Hill, 1941, pg. 295
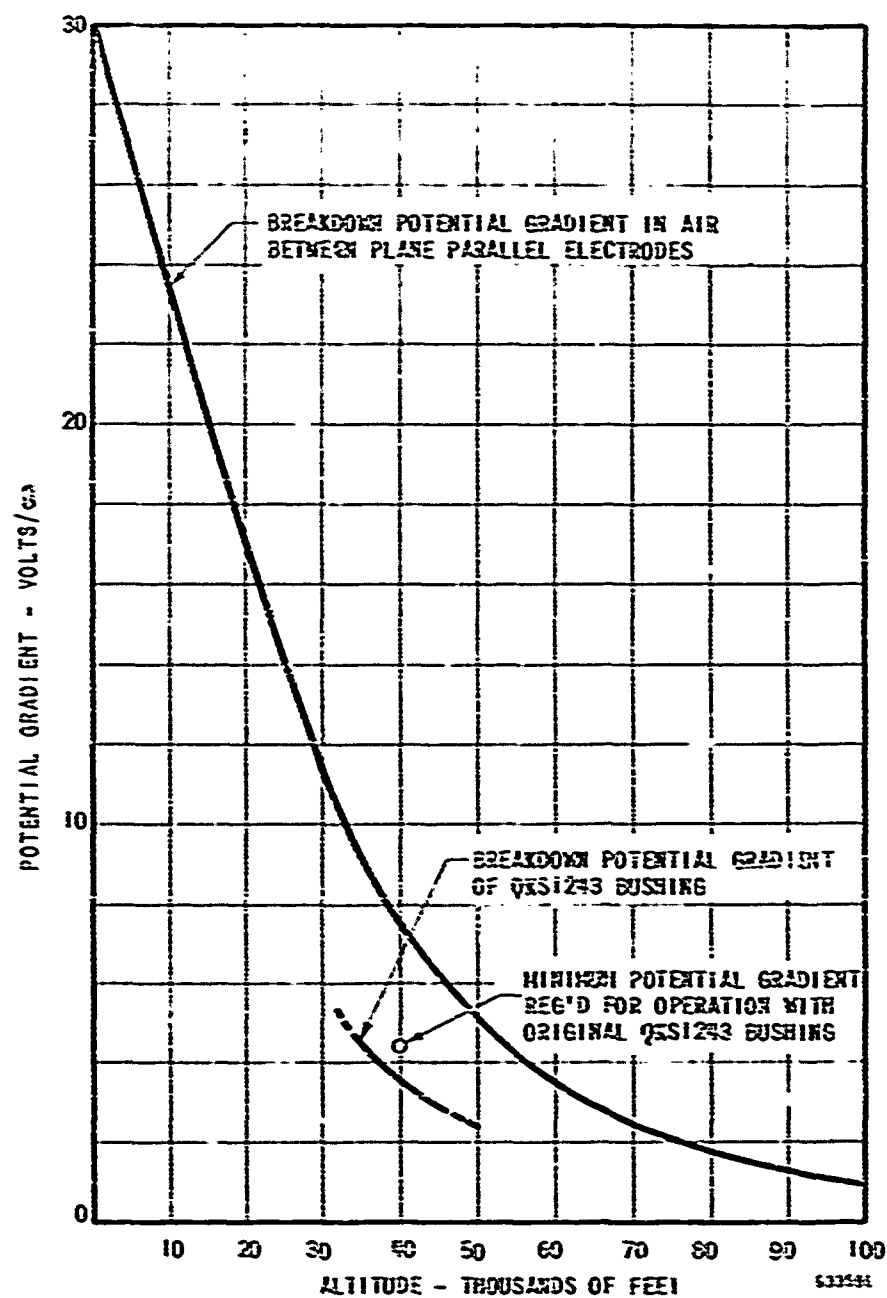
FIGURE 17   HIGH VOLTAGE BUSHING VOLTAGE BREAKDOWN

- 34 -
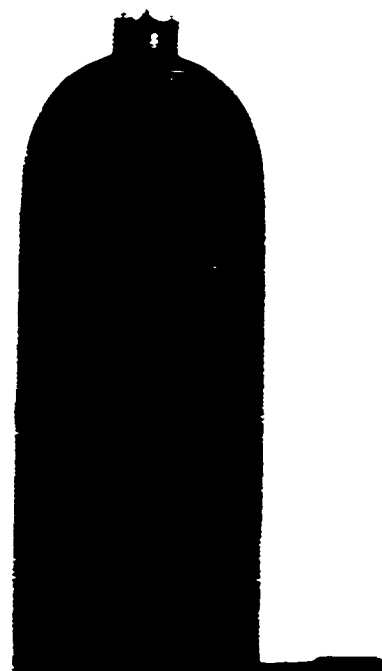
Figure 18 X-Ray Photograph - QKS1243 Potted Bushing

corona difficulties would be encountered unless a path to ground was provided. A measure of success was attained with the design of Figure 18, yet it was abandoned for the following reasons.

(a) Air bubbles occluded in the potting compound resulted in dielectric breakdown and consequent failure. This problem could have been solved by improvement of the potting technique.

(b) No connector was commercially available to connect the flying lead to the pulse transformer.

(c) The potting and metallic grounding required to prevent corona increased the A-K capacitance from 11.5 to 82 pf. Although the latter could have been reduced in the final design, there would always be a large capacitance.

5.2.8.4 Based upon the above results, it appeared that the best approach to the voltage breakdown problem would be to partially pressurize the input bushing. Accordingly, further efforts at potting were dropped.

5.2.9 Design for Vibration

5.2.9.1 Three sensitive areas exist to which attention must be paid in achieving a vibration-proof tube design. First, since a tube is usually supported from bolts which pass through the permanent magnet, it is desirable to have a four-point connection with each point removed from the tube axis as far as possible and equally spaced in azimuth. This scheme was adopted for the low power stage (QKS1244). However, a different design was available for the QKS1243 from the prototype Amplitron. This design (see Figure 9) provides two bolts passing through the magnet for primary support. Auxiliary support to a surface co-planar with the edge of the magnet and parallel to the plane of the bolts is also required.

- 36 -

5.2.9 2   The second area of importance concerns the minimization of relative motion between the anode assembly and the magnet, and the waveguide flanges with respect to the magnet.   A technique which aids in the latter and at the same time prevents deformation of the waveguide due to physical handling is the provision of short supporting struts between the flange and the magnet.   These struts are brazed to the waveguide and project into holes in the magnet, where they are secured with epoxy.   The same epoxy (Bigg's #460) used to pot the two holes in the magnet which encloses the tube body keeps the latter rigid with respect to the magnet.   In use, additional supports between the waveguide flanges and the equipment frame will be required.

5.2.9.3   The third area of importance, which required considerable engineering, was the development of a cantilever cathode design which would withstand the required vibration.   The initial design, from the QKS506 Amplitron, showed mechanical resonances at 115 cycles and at 180 cycles.   A number of changes were required to achieve a design good to 500 cycles.   These were guided by the general principle of obtaining a geometrical cone of tapered mass. In the end the design was completely changed mechanically.   Several joints, which were previously welded, were changed to brazed joints.   The test of the final design shown in Figure 17 was resonance-free up to 850 cycles.

5.2.10   QKS1243 Hot Tubes

5.2.10.1   For the record, Table III presents design and process information for each of the QKS1243 tubes built during the program.
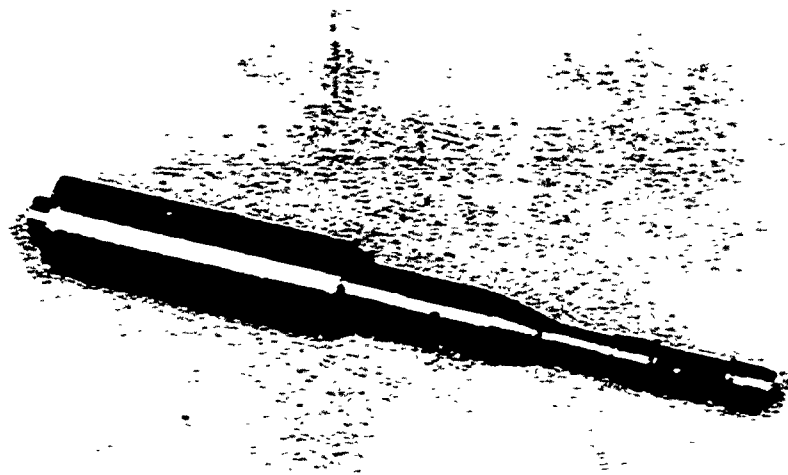
64 2-322

Figure 19 Photograph - QKS1243 Ruggedized Cathode

TABLE III

QKS1243 CONSTRUCTION DATA

Tube No.	da	dc	h	Bakeout 8 hrs at 450°C	Getter Outgas at 1.0 Volt	Disposition
A	.500	.300	.616	12.5 hrs at 450°C	10 amp	Failed - Window Weld
B	.480	.280	.616	24 hrs at 460°C	10 amp	Scrapped
C	.480	.280	.616	24 hrs at 480°C	10.5 amp	Life test
D	.480	.280	.616	18 hrs at 480°C	10.1 amp	Failed - Window Weld
E	.490	.280	.616	17 hrs at 460°C	10.0 amp	Chain #2
F	.492	.280	.616	19.5 hrs at 460°C	10.1 amp	Chain #3
G	.492	.280	.616	20.5 hrs at 460°C	10.0 amp	Chain #4

5.3 Development of the QKS1244 Amplitron

5.3.1 Design Parameters

5.3.1.1 The final parameters for the interaction space design of the QKS1244 are presented in Table IV below

TABLE IV

QKS1244 DESIGN PARAMETERS

Band Center Frequency, fo	9.6 Gc
Number of active network sections, S	16
Drift section length (in network pitches), k	2
Network pitch, p	0.0506
Space charge mode number, n	7
Anode diameter, da	0.290 in
Cathode diameter, dc	0.178 in

Characteristic voltage, Vo	2850 volts
Characteristic magnetic field, Bo	1555 gauss
Characteristic power, Po	48.7 kw
Approximate B/Bo ratio	3.28
Operating voltage	16.0 kv
Interaction space length, h	0.282 in

5.3.2 Phase Frequency Characteristics of the Slow Wave Circuit

5.3.2.1 The methods of achieving and reproducing a proper phase shift characteristic were identical to those used for the higher powered stage. For record purposes Figure 20 shows the resonance plot for cluster 17 (used in QKS1244 #4) and Figure 21 shows the results of detailed phase shift measurements.

5.3.3 Matching

5.3.3.1 Matching of the slow wave circuit to uniform waveguide was accomplished by means of tapers from uniform guide to double-ridged waveguide, thence via parallel planes to the network straps. A representative match (obtained from QKS1244 #1 - Chain #4) is shown in Figure 22. Improvements of this match can be made as additional tubes are built.

5.3.3.2 During the development of the QKS1244 problems were caused by a drift section resonance which was very weakly coupled to the input waveguide but strongly coupled to the space-charge. The result of this resonance insofar as cold test was concerned was a very narrow band mismatch near 9300 Mc with an amplitude as low as 25% input reflection for a matched output. Yet, at hot test, power would be generated at this frequency and little of it would be propagated to the output. The end result was low gain and low efficiency.
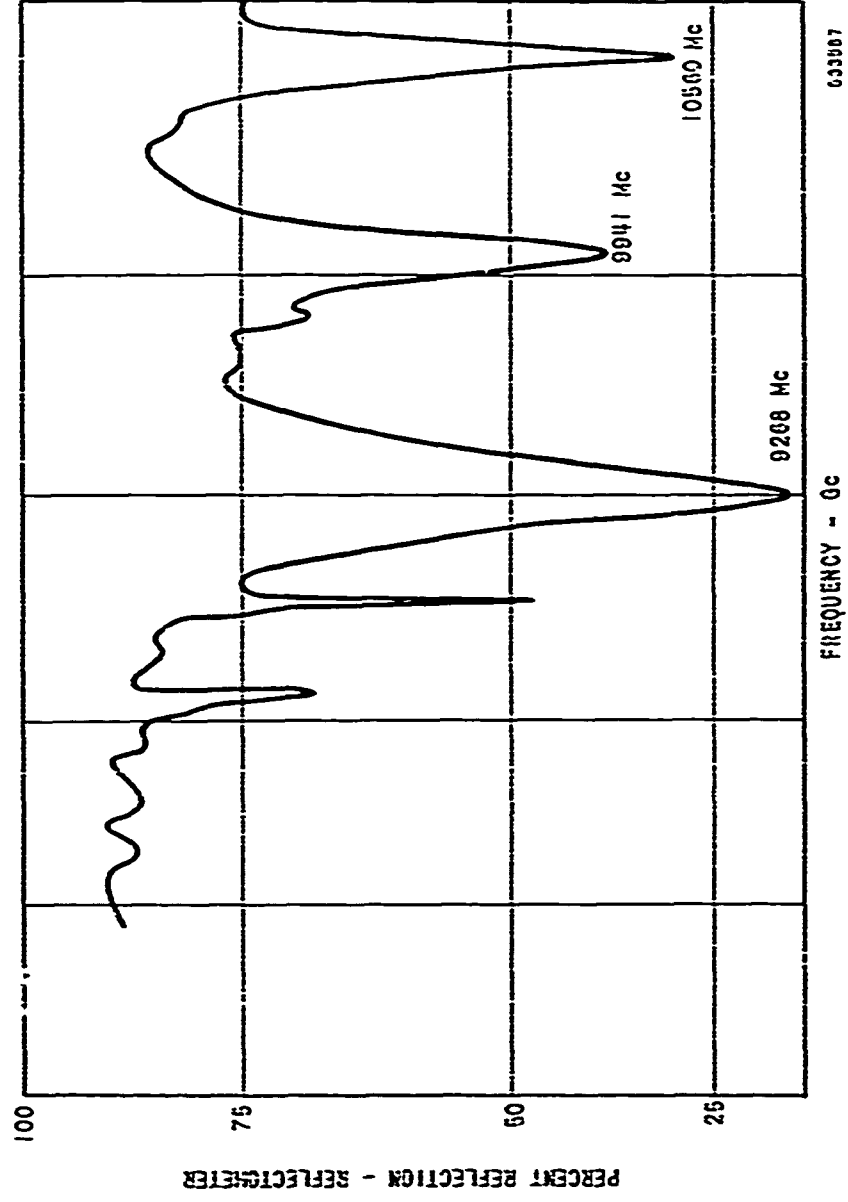
RESONANCE PLOT QKS1244 (CLUSTER#17)
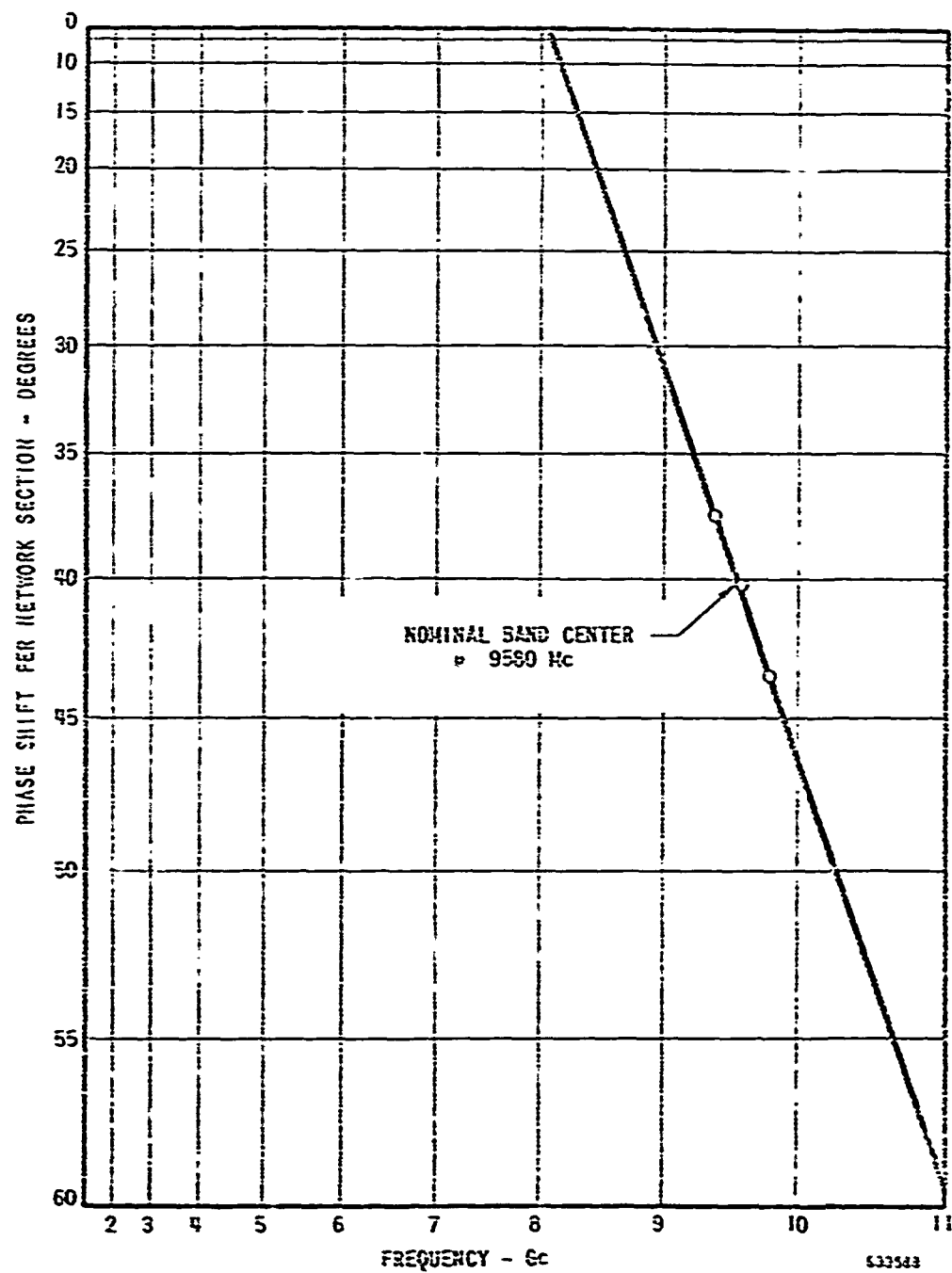
FIGURE 20

FIGURE 21   QKS1244   CLUSTER #17   PHASE DATA

- 42 -
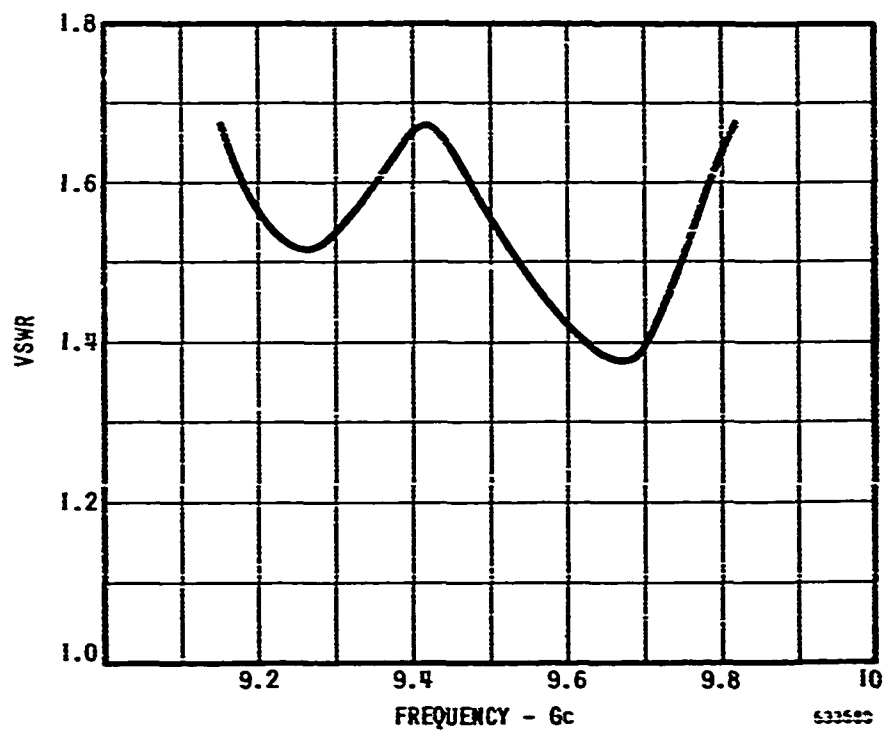
FIGURE 22   INPUT VSWR vs FREQUENCY QKS1244 #4
(HATCHED TERMINATION)

- 43 -

5.3.3.3   In overcoming the problem a large number of experiments were required.   These were described in the interim reports.   In the end. a cure was devised whereby a strap-like member was bridged across the drift section to decouple the resonance from the space charge.

5.3.4   RF Window

5.3.4.1   The rf windows used for the QKS1244 Amplitron are identical to those developed for the QKS1243.

5.3.5   Cold Cathode Operation

5.3.5.1   At the outset it had been expected that cold cathode operation of the QKS1244 would be achievable.   During the course of the program. however, it became evident that such operation, although generally successful, would not be reliable enough to be specified.   The problem relates to the relatively low peak rf drive power available and to the low back-bombardment power being fed to the cathode structure.   Because of the latter, any accidental application of overvoltage to the tube (as for example, might result from a trigger misalignment) results in a condition whereby the cathode quickly becomes poisoned.   To overcome this possibility, it was necessary to specify 10 watts of heater power to ensure that the poisoning phenomenon would not easily take place.

5.3.6   Cooling Analysis

5.3.6.1   The QKS1244 Amplitron, like the QKS1243, was to meet the requirements of MiL-E-5400 for Class 1 equipment, but to an altitude of 40,000 feet.   It assumed that for satisfactory cooling the hot spot on the external surface of the anode must be less than $125^{\circ}C$ and the hot spot on the internal surface of the anode must be less than $450^{\circ}C$, for the $31^{\circ}C$ air temperature.   The total dissipation at the anode was assumed to be 84 watts (56 watts output at 40% efficiency.)

Details of the internal anode structure were not considered, because it was known that with usual construction the internal anode copper hot spot would be much less than $450^{\circ}C$

5.3.6.2   The external design of the tube consists of a 1 1/2 in. diameter anode cylinder brazed into a piece of 1 1/4 or 5/8 inch copper waveguide, with 1/16 inch wall thickness, and of 6 inch length   The whole assembly is surrounded by a boxal magnet through which the two waveguide ends protrude. (See Figure 9).

5.3.6.3   Preliminary computations indicated that natural cooling means were inadequate, but that the waveguide had sufficient conductance so that its surface can be used for heat exchange by forced convection   It was decided that the magnet be used as a plenum chamber with air being supplied by blower or ducting from an air supply through holes in the magnet   The air would exhaust through four finned heat exchange sections on the waveguide at the openings in the magnet   The finned sections would be brazed or soldered onto the wide surface of the waveguide as shown by Figure 9

5.3.6.4   The fin copper thickness represents a compromise between fin effectiveness and air flow resistance   The fin spacing represents a compromise between cooling and dust collection; if the air were clean a moderately larger number of corrugations could be used.

Computations were made of required total air flow and resulting total pressure drop for the finned sections   The least effective design (12 corrugations) was assumed for these computations.   It was also assumed that pressure loss at the blower entrance through the magnet would be small (requiring a cross-section of at least 2 square inches) and that air leakage out of the magnet (other than through the fins) would be negligible.   A blower found to be suitable was the Aximax 3 with 387JS motor.   At 40,000 feet altitude this was computed to just meet the requirements (44 CFM 0 60 lb/min . 0.7 H_2O), while cooling at lower altitudes was slightly in excess of requirements.

- 45 -

5.3.6.5 An Aximax 3 with 500 JS motor would provide better cooling over the full altitude range, but uses slightly more power (less slip) at low altitud An Aximax 2 with 305JS motor is moderately undersized over the full altitude range and may be adequate if the anode dissipation is less than 84 watts.

5.3.7 Design for Vibration

5.3.7.1 No problems were encountered in preparing the QKS1244 for vibration. The newly designed permanent magnet was bowl-shaped (see Figure 23) to provide a four-point mounting arrangement. The sides of the bowls were made to enclose and support the input and output waveguides. A firm bond between the tube and the magnet was assured by the use of epoxy around the input bushing base, the exhaust end of the tube and the two waveguides as they passed through the magnet. The cathode, which is smaller and shorter than that of the QKS1243, posed no design problems.

5.3.8 QKS1244 Tubes

5.3.8.1 Table V presents pertinent information for each of the QKS1244 tubes built during the program

Table V

QKS1244 Construction Data

Tube No.	da	dc	h	Bakeout	Getter Outgas	Disposition
A	.264	.151	.296	18 hrs at 450°C	1.4 volts 5.5 amps	Scrap
A-1	.264	.160	.295	8 at 400		Scrap
A-2	.264	.160	250	15.5 at 400		Scrap
B	.264			8.5 at 450		Scrap
B-1	264			8 at 450		Scrap
B-2	.264					Scrap
B-3	.264					Scrap
C	.254	.162	250	8.5 at 450		Scrap

- 4 -

Figure 23   Outline Drawing QKS1244

OBJECTIVE

Best Available Copy

TABLE V (Continued)

Tube No.	da	dc	h	Bakeout	Getter Outgas	Disposition
C-1	.264	.149	.280	6 hrs at 450°C		Scrap
C-2	.264	.149	.250			Scrap
D	.264	.162	.280			Scrap
D-1	.264	.175	280			Scrap
E	.290	.177	.280			Scrap
E-1	.290	.177	.280	18 at 460	1.6 - 4.5	Chain #3
F	.290	.178	.280	8.5 at 450		Scrap
G	.290	.178	.280	16.0 at 460	4.0	Chain #2
H	.290	.177	.280	8.5 at 450	4.8	Life Test
I	.290	.178	.280	23 at 460	4.5	Chain #4

5.4   Chain Performance
       5.4.1   Test Facilities

5.4.1.1   Four test modulators were used at various times during
the QKS1243/1244 program.   Three were line type modulators and one was a
hard tube modulator.   The test area is illustrated by Figure 24.   The line modula-
tors were used to operate a special 1 kw magnetron at 2.4 µs, the QKS1244 at
2.2 µs and the QKS1243 at 2.0 µs all from a common, delayed trigger generator.
The hard tube modulator provided the means of processing both a QKS1243 and a
QKS1244 simultaneously.   For vibration testing the three line type modulators
were moved into the environmental test laboratory.   In the main test area a screen
room was available within which spectral power measurements were made with a
Polarad FIM receiver.

5.4.1.2   Phase measurements were made using a conventional wave-
guide loop technique as shown by Figure 25.   Difficulty was experienced with
crossguide couplers in that the phase of the output wave did not track from one
coupler to the next of the same type.   The problem is exemplified by the data of
Figure 26, in which the phase difference between the output arm of one coupler
and the output arm of a similar coupler has been plotted as a function of frequency
The inability of these couplers to track plus other lesser factors which contribute
to calibration curve deviation from linearity, results in a condition where calibra-
tion errors are of the same order of magnitude as the phase differences being
measured.   Although the data presented for the tube chains show clearly that they

- 48 -
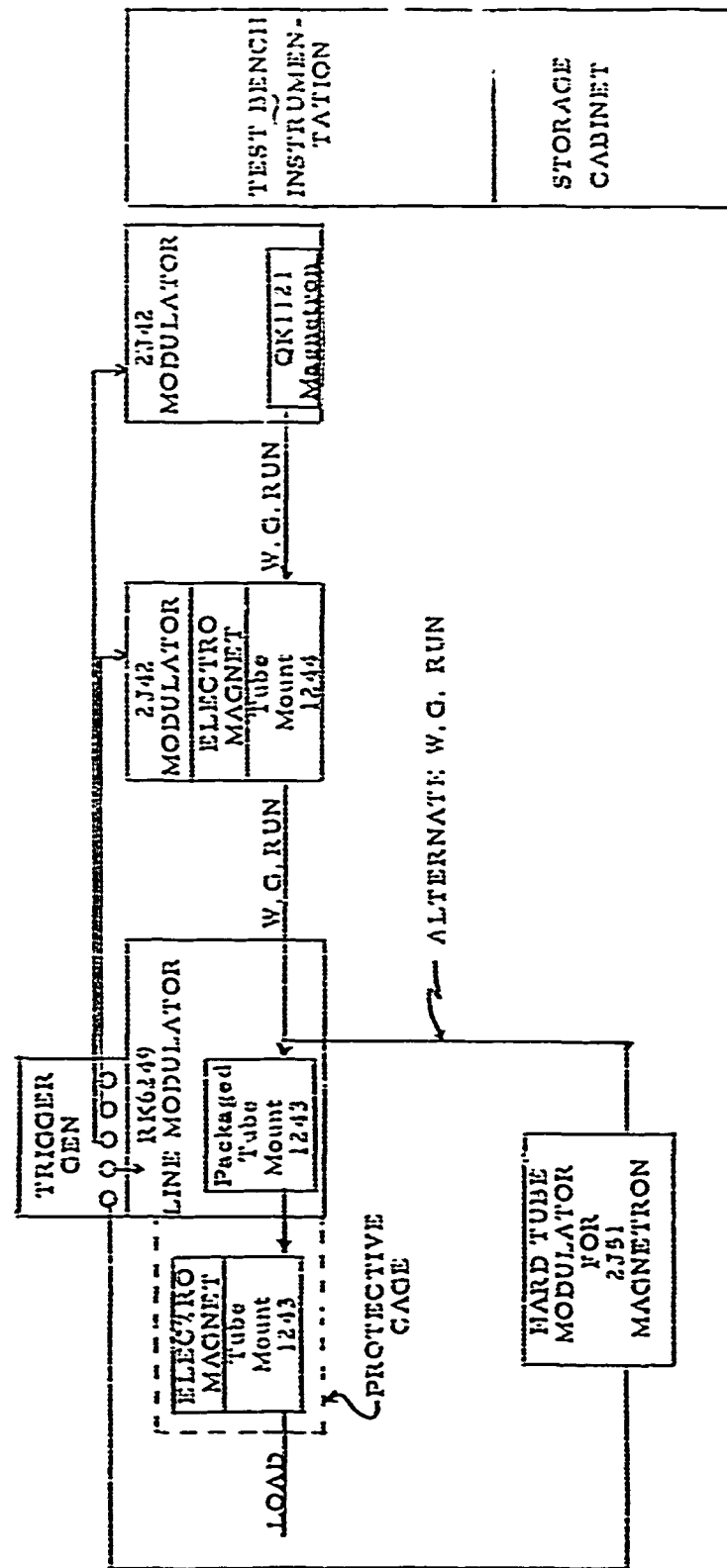
Figure 24 QKS1243/1244 TEST AREA

030003

- 58 -
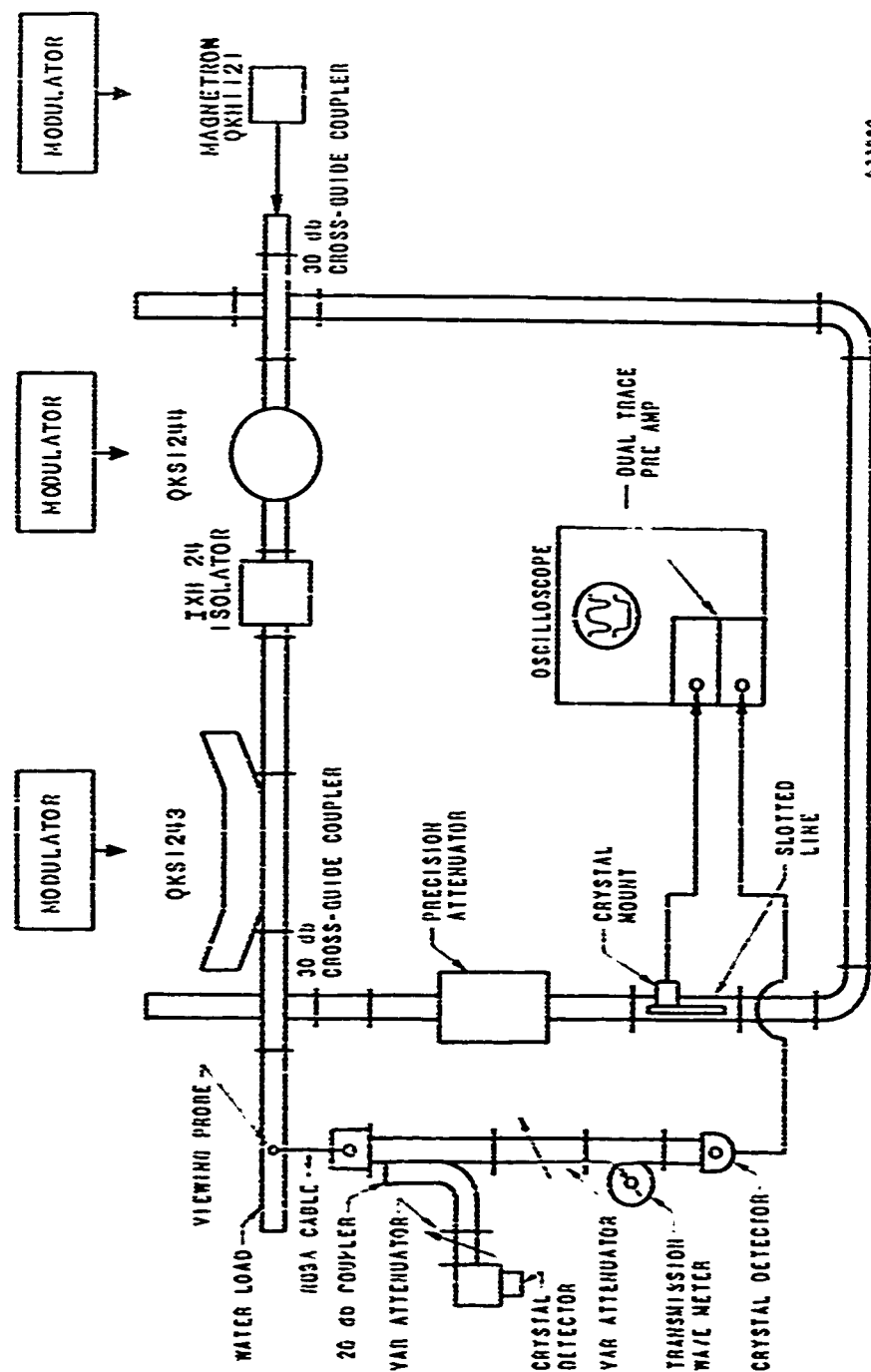
TEST SETUP FOR PHASE MEASUREMENTS
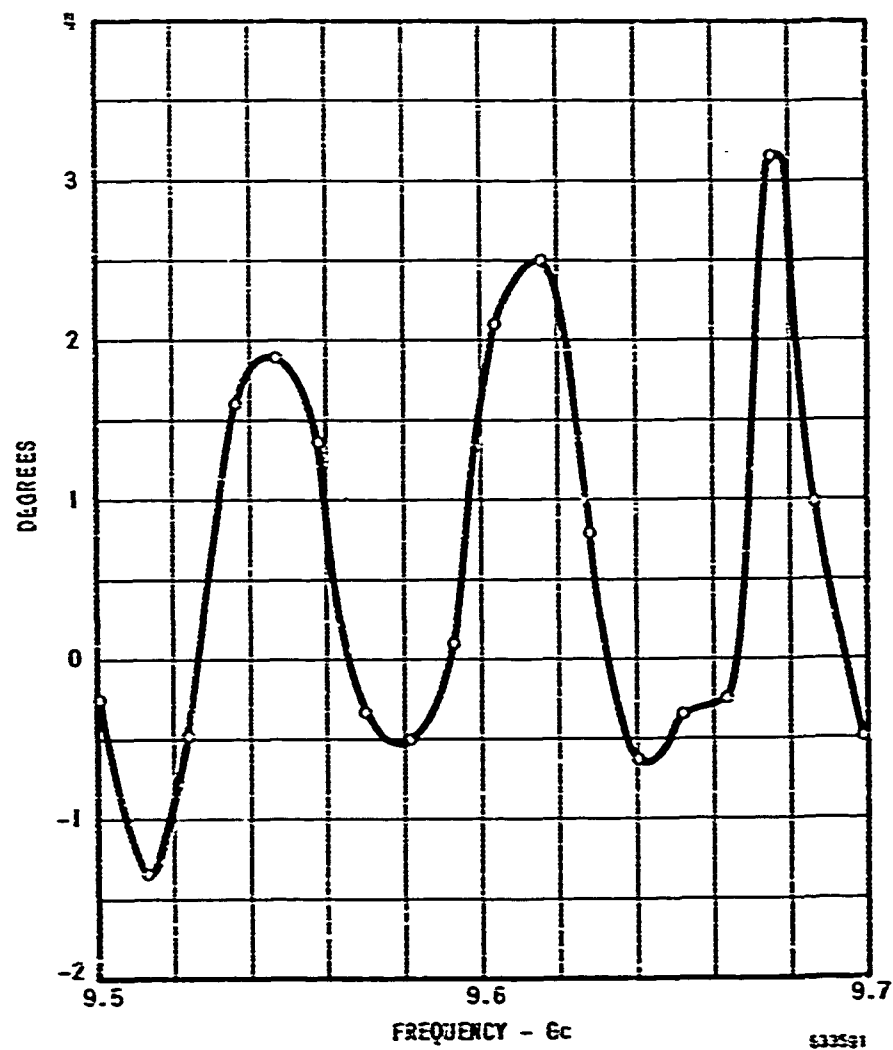
FIGURE 2B

FIGURE 26   DIFFERENCE BETWEEN THE PHASE vs FREQUENCY
CURVES OF 30 db COUPLERS #243 AND #244

meet the specifications, it is believed that many of the apparent variations are illusions caused by the test setup. Another source of error in the phase linearity measurements was caused by long term line variations and thermal drift. Through the phase sensitivity of the tubes such long term variations can produce the illusion of phase variations that do not exist. Thus, it is expected that the system response under actual conditions will be better than that predicted from the test data.

5.4.2   Vibration Tests

5.4.2.1   As explained in the tube development sections auxiliary support is necessary for the tubes in the following areas before they will endure vibration successfully:

> (a)   The waveguide flanges
>
> (b)   In a plane parallel to that which includes the mounting bolts of the QKS1243.

5.4.2.2   The above recommendations were determined experimentally. Because they were not wholly anticipated when the vibration test fixture was first procured, the fixture became rather awkward. Nevertheless, Figures 27 through 31 showing several views of the test fixture, illustrate the general types of auxiliary supports required. Figure 27 shows an over-all view of the test setup including the following:

> (a)   The modulators and electrical controls
>
> (b)   The vibration test console
>
> (c)   The tubes and vibration fixture
>
> (d)   A strobe light for visual observation of the vibration
>
> (e)   A scope displaying the rectified rf output pulse.

Figure 27
QKS1243/1244 Vibration Test Setup
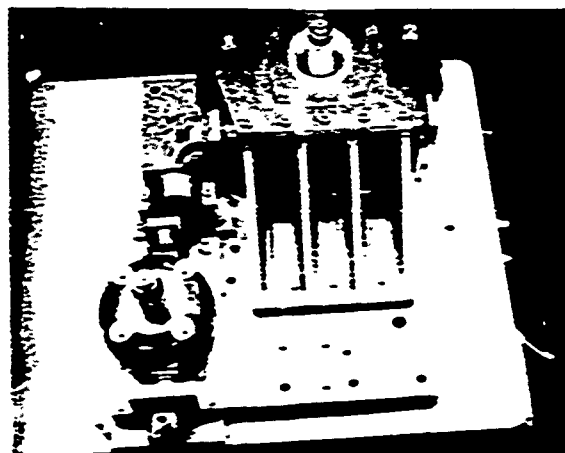
Figure 28
Plan View - Vibration Test Fixture
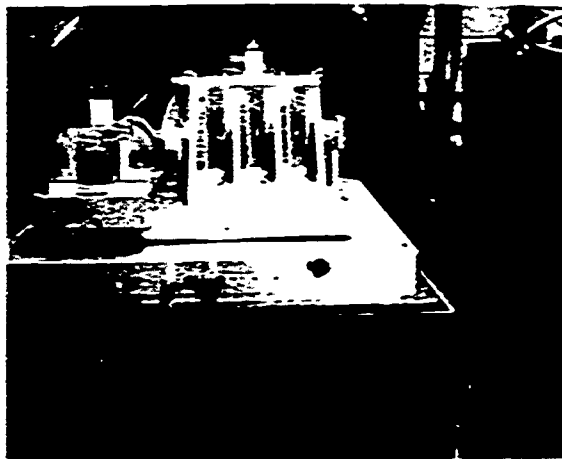
Figure 29
Vibration Setup - Side 1

Figure 30
Vibration Setup - Side 2
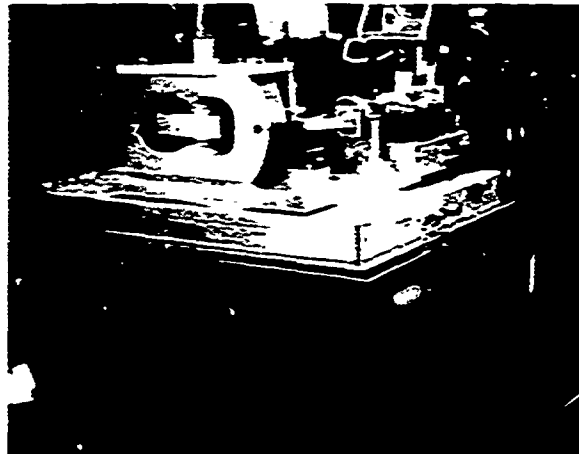
Figure 31
Vibration Setup - Side 3
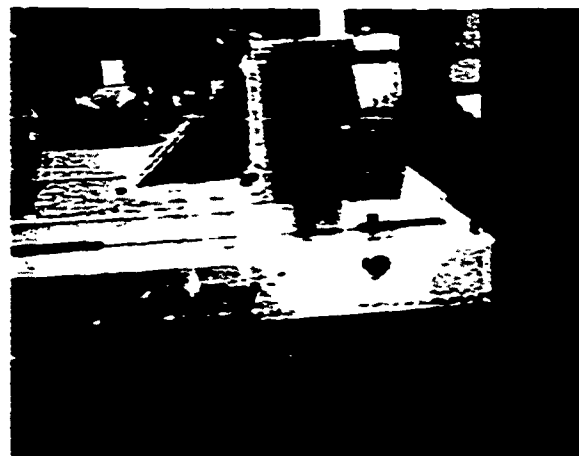
Figure 32
Vibration Setup - Side 4

5.4.2.3 Details of the mount are in Figure 25, a plan view of the main mounting

(a) The rf input by means of a coaxial-waveguide adapter

(b) A clamp on the rf input flange

(c) A clamp on the interstage isolator which in this setup had to be adjacent to the QKS1244[5]

(d) Waveguide flange supports on both ends of the QKS1243

(e) Auxiliary support for the QKS1243 to prevent vibration in the direction of the QKS1244 waveguide run. (See Figure 30.)

Figures . through . show additional views of all four sides of the vibration test fixture proceeding in a clockwise direction. These indicate how the restricted area of the main vibration plate prevented simple support of the QKS1243 by a surface bearing against the magnet and forced the rather awkward support actually used.

5.4.2.4 With the tube chain operating under rated conditions vibration tests were performed at 10 g to 500 cycles per the requirement of MIL-E-5400. These tests performed in each of three mutually perpendicular planes were wholly successful in that no resonances were apparent under the strobe light and no amplitude oscillations were apparent in the rectified rf pulse. Calibration of the scope in db was made possible by the inclusion of a calibrated attenuator in the rf line.

5.4.3 Life Test

5.4.3 1 As required in the contract, one tube chain was life tested for 300 hours, 150 hours under the low duty cycle conditions and 150 hours under the high duty cycle conditions. Tubes QKS1243 #C and QKS1244 #H were selected for this purpose. Although this chain was operable under standard conditions, i e., at the same operating point as for those tubes shipped, the chain was low in

---

5 For freedom of interaction between the various magnet fields waveguide runs of 1.7 inch and 4.0 inches are recommended between the isolator and the QKS1244 and QKS1243, respectively.

power output. The low power output, however, with normal power input was felt to yield a more severe and thus more fruitful life test because of the greater anode dissipation.

5.4.3.2 No problems were encountered during the test. The tubes were tested both before and after the 300-hour period to check for a change in the upper mode boundary. It was found to be unchanged. The only change observed was in the power output which declined 6% over the first 40 hours and thereafter remained reasonably constant. Such a decline during the initial period of life is commonly observed in high power tubes and in no way indicates a short lifetime In Figure 33 the power output variation with time is shown with a compilation of the conditions of operation.

5.4.4 Phase Sensitivity

5.4.4.1 The technical requirements called for the amplifier chains to have no more than a 1.5 degree phase variation for a 1.0 percent variation of pulse power. Actual testing to this specification was not possible because:

   (a)   the amplifier chain was made of two tubes and an isolator. Each tube was operated from its own pulse modulator and power supply. Therefore there was no convenient way to vary the pulse power input to the two tubes simultaneously in a controlled fashion.

   (b)   two terminal crossed-field amplifiers are more amenable to testing in terms of current variations because of their biased diode type of V-I characteristic.

5.4.4.2 A relationship between the phase sensitivity to current and that to pulse power can be derived as follows

$$dP = VdI \div I dV$$
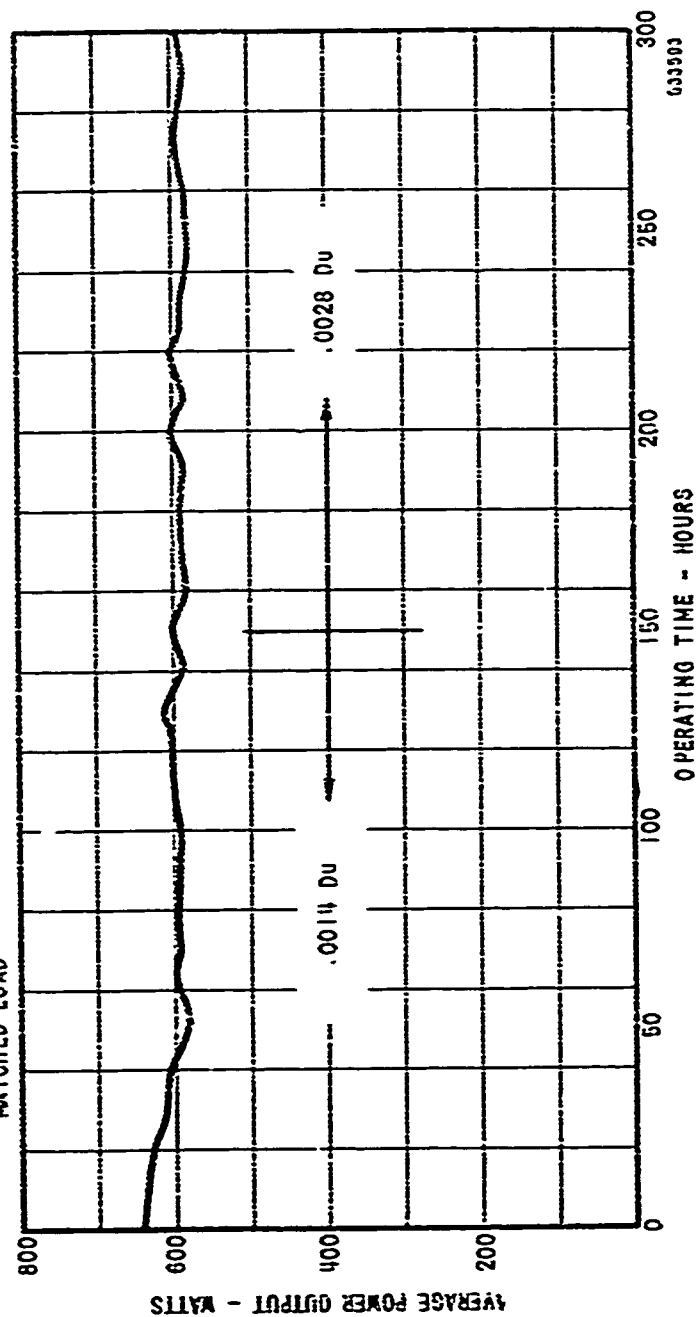
$$\frac{dP}{P} = \frac{dI}{I} \div \frac{dV}{V}$$

POWER OUTPUT vs TIME
QKS1243/1244 AMPLIFIER CHAIN #5
LIFE TEST

FIGURE 33

- 68 -

$$\frac{d\ell}{V} = \frac{Zd}{Zs} \qquad \frac{dI}{I} = \left[\frac{dV}{dI}\right] \left[\frac{I}{V}\right] \left[\frac{dI}{I}\right]$$

$$\frac{dP}{P} = \frac{dI}{I} \left[1 + \frac{Zd}{Zs}\right]$$

where

I = current

V = volt.

Zs = static impedance = V/I

Zd = dynamic impedance = dV/dI

Modulator power = V I

The ratio $\frac{Zd}{Zs}$ is ≈ 0.1 for Amplitrons. The power variation in terms of a 1.0 percent current variation is

$$\frac{dP}{P} = 1.0 \left[1 + 0.1\right] = 1.10$$

Therefore. $\Delta 9 = (1.1)(1.5) = 1.65$ degrees.

5.4.4.3 Because the Amplitron currents could not be varied simultaneously and in synchronism, the worst possible specification interpretation was used, that is,that the phase variations of each tube would add algebraically. In other words,the requirement was accepted that the sum of the phase variations of the QKS1243 and the QKS1244 be less than 1.65 degrees for a 1 percent change of Amplitron current.

5.4.4.4 Measurements of phase were made with the phase loop previously described. Using this technique the relationship between phase shift $\Delta\phi$ and the shift of minimum position Δx. is

$$\Delta\phi = \frac{2\Delta x}{\lambda_g} \times 360^\circ$$

In the test Δx was measured by means of a micrometer. For these measurements $\Delta\phi$ in terms of Δx was very close to 0.5 degrees per thousandth.

Exact values of the motion to phase factor were as follows:

(Mc)	$\Delta\phi/\Delta x$ (in degrees per thousandths)
9525	0.484
9600	0.490
9675	0.495

5.44.5 Results of the phase sensitivity measurements are given in Table V for the three chairs delivered, Numbers 2, 3 and 4.

Table VI
Results of the Phase Sensitivity Tests

Chain	Freq. Mc	QKS1243 .0014 du	QKS1243 .0028 du	QKS1244 .0014 du	QKS1244 .0028 du	Total .0014 du	Total .0028 du
#2							
#3	9501		0.435		0.18		.615
#4			0.50		0.51		1.01
#2			0.34		0.72		1.06
#3	9525	0.615		0.19		0.805	
#4		1.0		0.53		1.53	
#2		0.55	0.58	0.84		1.39	
#3	9600	0.48	0.72	0.39	0.26	0.87	0.98
#4		0.81	1.05	0.42	0.33	1.23	1.38
#2			0.47		0.90		1.37
#3	9675	0.56		0.18		0.74	
#4							
#2							
#3	9699		0.695		0.22		0.915
#4		0.71	0.415	0.33	0.35	1.06	0.765
Average		.675	.578	.413	.434	1.10	

5.4.5 Discussion of Results

5.4.5.1 The phase sensitivity of a TWT can be expressed as

$$\Delta\phi = 0.36 \frac{\Delta V}{V}$$

where ϕ is the total electrical length in degrees and is equal to 360 times the number of beam wavelengths N.

For comparison, we shall postulate that for an Amplitron $\Delta\phi = 0.2\,\phi\,\frac{\Delta V}{V}$ and see first whether or not the measured data fit this relationship and secondly how the Amplitron's sensitivity would compare with that of a comparable TWT.

5.4.5.2 Because the Amplitron uses a backward-wave circuit, the number of beam wavelengths can be large when the slow-wave circuit is actually short. For example, in the QKS1243, the circuit length is 2.0 wavelengths, whereas there are 8 beam wavelengths. These numbers are obtained using the notation of Section 4.0, as follows $\frac{\ell}{\lambda}$ = circuit wavelengths = $\frac{S(\pi-\beta_0 P)}{360}$, beam wavelength = n = $\frac{(S+k)\beta_0 P}{360}$, where β_0 is the phase shift at band center.

The quantity $(\pi - \beta p)$ is that which is illustrated in Figures 12 and 11. For the QKS1243, from Figure 11 $(\pi - \beta_0 p) = 36°$

$$\frac{\ell}{\lambda} = \frac{18 \times 36}{360} = 1.8$$

and

$$n = \frac{20 \times 144}{360} = 8.$$

5.4.5.3   Referring to the table of results the QKS1243 phase sensitivity averages are 0.675 for the .0014 duty cycle and 0.578 for the high duty cycle for a mean value of .627   Similarly the mean of the QKS1244 average values of .413 and .434 is .424   We shall check the fit of these in our postulated relation First. however we wish to express phase sensitivity in term of current.   For the Amplitron.

$$\frac{dI}{I} = \frac{Z_s}{Z_d} \left(\frac{dV}{V} \right) \cong 10 \left(\frac{dV}{V} \right)$$

and for the TWT (cathode pulsed)

$$I = KV^{3/2}$$

$$dI = \frac{3}{2} KV^{1/2} dV$$

$$\frac{dI}{I} = \frac{3}{2} \left\{ \frac{KV^{3/2}}{I} \right\} \frac{dV}{V} = \frac{3}{2} \left(\frac{dV}{V} \right)$$

$$\frac{dI}{I} = \frac{3}{2} \left(\frac{dV}{V} \right)$$

Now the phase sensitivity formulae become

<table>
<tr><td>TWT</td><td>AMPLITRON</td></tr>
<tr><td>$\Delta\phi = 0.3 \phi \frac{\Delta V}{V}$</td><td>$\Delta\phi = 0.2 \phi \frac{\Delta V}{V}$</td></tr>
<tr><td>(1)</td><td>(2)</td></tr>
<tr><td>$\Delta\phi = 0.2 \phi \frac{\Delta I}{I}$</td><td>$\Delta\phi = 0.002 \phi \frac{\Delta I}{I}$</td></tr>
</table>

and for various Amplitrons

	$\Delta\phi$ Calculated	$\Delta\phi$ Measured
QKS1243	0 575	0 627
QKS1244	0 504	0 424
QKS434	0 283	0 270
QKS1286	0 504	0 403
QKS622	0 704	0 250
QKS681	0 288	0 500

These data indicate that use of the relationships (2) will predict Amplitron phase sensitivity within a factor of two. It may, therefore, be most useful in system planning or, as will be seen, for comparison.

5.4 5 4   It is of interest to compare the phase sensitivity of the QKS1243, 1244 amplifier chain to a comparable TWT. At X-band a TWT with 27 db gain has approximately 18 beam wavelengths. Its phase sensitivity to voltage and current changes of 1 0 percent are shown below

	Voltage Variation	Current Variation
TWT	19 4	13 0
Amplitron	10 8	1.05
Improvement Factor (Amplitron over TWT)	2	13[o]

5.4 6   Phase Linearity of a Dispersive Amplifier

The slow-wave network of an Amplitron is usually dispersive, i e , the group velocity v_g is not equal to the phase velocity v_p in the frequency band of interest. However, its phase-frequency characteristics can usually be approximated by a straight line of form $\phi = \phi_o + b_o x$. Because there has been some

---

[o]   The gridded TWT has a sensitivity to current in the order of $\Delta\phi = 0$ 1 o $\frac{\Delta I}{I}$ and thus the Amplitron/TWT improvement factor would be only 6 5 when compared to a gridded tube

confusion as to the effect of θ_o on transmission distortion. this is investigated in the following two ways:

(a) Given an input signal[6]

$$(1) \quad G(t) = \frac{1}{2\pi} \int_{-\infty}^{\infty} S(\omega) \, \epsilon^{j\left[\omega t \, + \, \phi_{(\omega)}\right]} \, d\omega$$

and a network with transfer function $A(\omega) \epsilon^{jB_{(\omega)}}$ where $A(\omega) = \frac{a_o}{2}$ and $B(\omega) = \theta_o + b_o \omega$ the output signal will be:

$$(2) \quad \overline{G}(t) = \frac{1}{2\pi} \int_{-\infty}^{\infty} S(\omega) \frac{a_o}{2} \, \epsilon^{j\left[\omega t \, + \, \phi_{(\omega)} \, + \, \theta_o \, + \, b_o \omega\right]} \, d\omega$$

$$(3) \quad \overline{G}(t) = A(\omega) \, \epsilon^{j\theta_o} \, G\left(t - b_o\right)$$

Equation (3) states that the output signal will be a replica of the input signal except that it will be delayed by time b_o, and amplified by the constant factor $\frac{a_o}{2}$ shifted in phase by the constant amount θ_o.

$$(b) \qquad \phi = \theta_o + b_c \omega$$

$$\frac{d\phi}{d\omega} = b_o \equiv \tau_g$$

τ = the time delay of transported energy in length $Z = \frac{Z}{\tau_g}$.

6 See "Frequency Analysis. Modulation and Noise". S Goldman. McGraw Hill. 1948 p 102

Thus, a dispersive network with linear phase will provide distortion free trans-
mission and pure time (energy) delay even though the phase time delay given by
$\frac{Z}{v_g}$ is a function of frequency

5.4.7 Amplitude and Phase Versus Frequency

5.4.7.1   During the program great interest was indicated in the
attainment of a linear phase - frequency characteristic. Hence the data measured
on each of the 3 delivered chains are reproduced herein.   These data appear as
plots of standing wave minima versus frequency   They are easily interpreted
since to a first approximation 0.002 inches is equal to 1.0 degree.   The plots,
Figures 31 through 39, show in most cases linearity within 4 degrees.   Only
in a few instances was the extra latitude permitted for a half cycle sinusoidal
component utilized

5.4.7.2 The phase loop calibration curve, (See Figure 40) when applied to the
uncorrected phase curves tends to straighten them out and makes the results
better.   Yet, in spite of the satisfactory results it is believed that the radar
system response will be even better because long term measurement errors due
to voltage drift and thermal drift will not be present and the errors inherent in
an X-band slotted line measurement of standing wave minima will be eliminated.
We say this because analysis of the Amplitron indicates considerably smaller
phase variations than those actually observed.   However, in any case, the phase
behavior of the three chains delivered is unquestionably good.

5.4.7 3   The output amplitude versus frequency characteristic of
a QKS1243/1244 amplifier chain can be expected to be quite flat with a downward
linear trend as frequency increases.   Power output versus frequency character-
istics for chains #3 and #4 are plotted on an expanded scale in Figures 41 and 42
These illustrate that the variable component is basically linear. The plots show
that, whereas the total deviation from pure flatness is at worst only 0 59 db,
the cyclic components have a peak-to-peak amplitude of only 0.08 db   These
data were obtained at constant setting of a line-type modulator, the only variable
being rf drive frequency
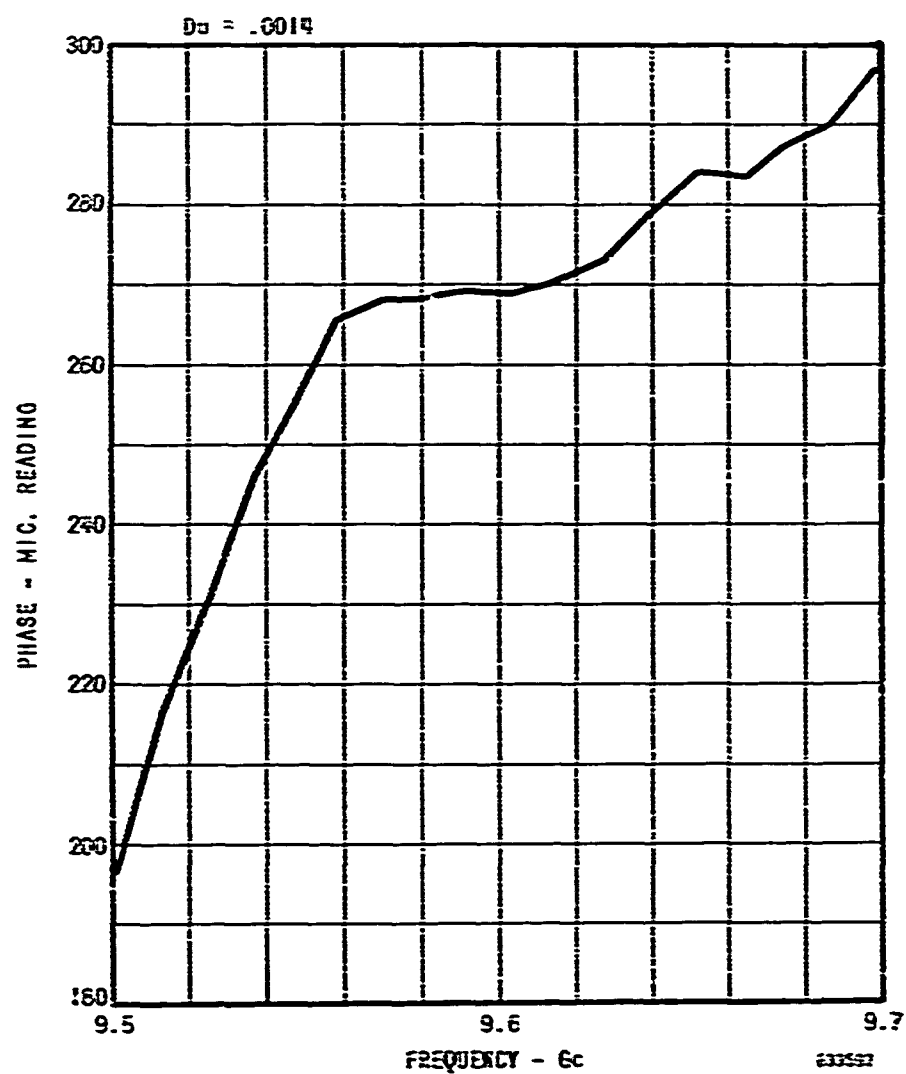
FIGURE 34   PHASE vs FREQUENCY QXS1243/1244 CHAIN #2
(uncorrected)

FIGURE 36   PHASE vs FREQUENCY CKS1243/1244 CHAIN #2
(uncorrected)

- 67 -

FIGURE 36   PHASE vs FREQUENCY QKS1243/1244   CHAIN #3
(uncorrected)
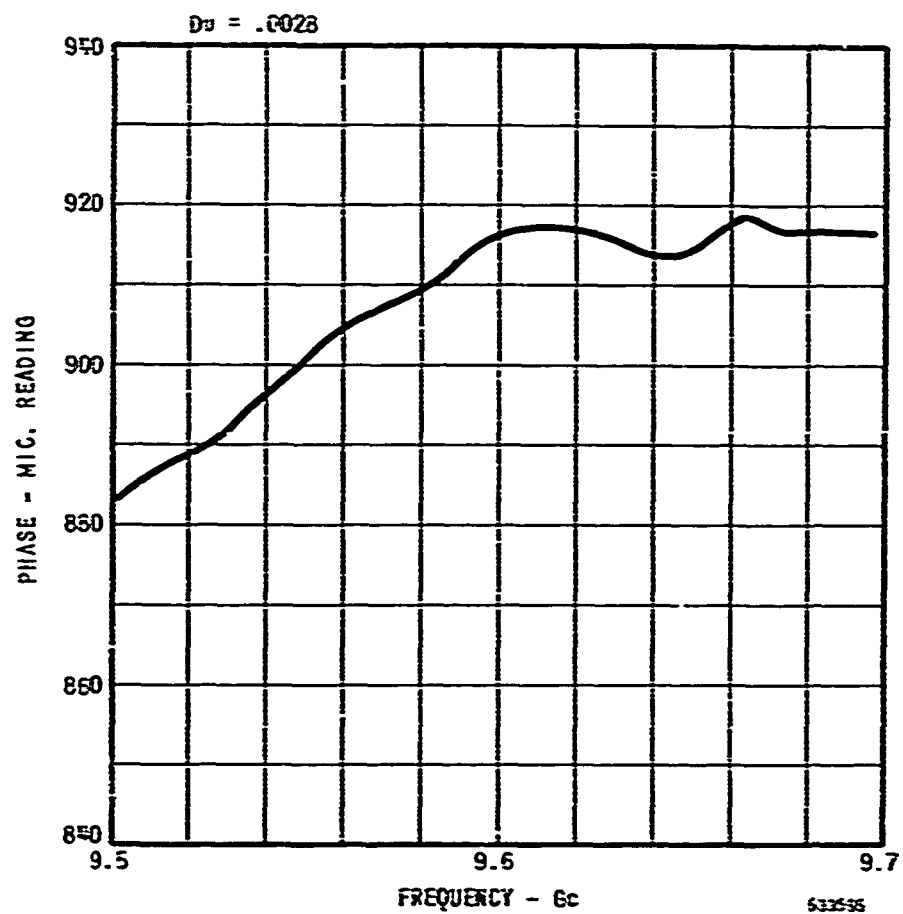
FIGURE 37   PHASE VS FREQUENCY QX>:243/1244 CHAIN #3
(uncorrected)
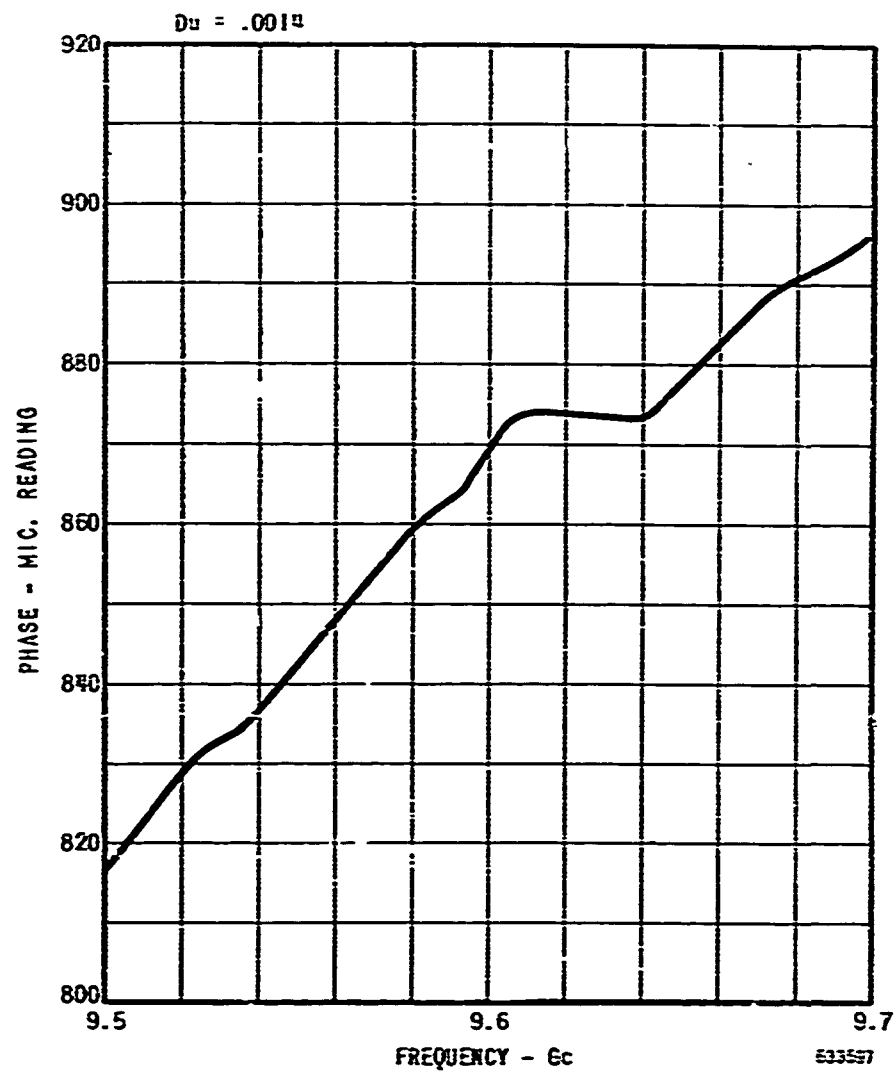
FIGURE 38   PHASE vs FREQUENCY   QKS1243/1244   CHAIN #4
(uncorrected)
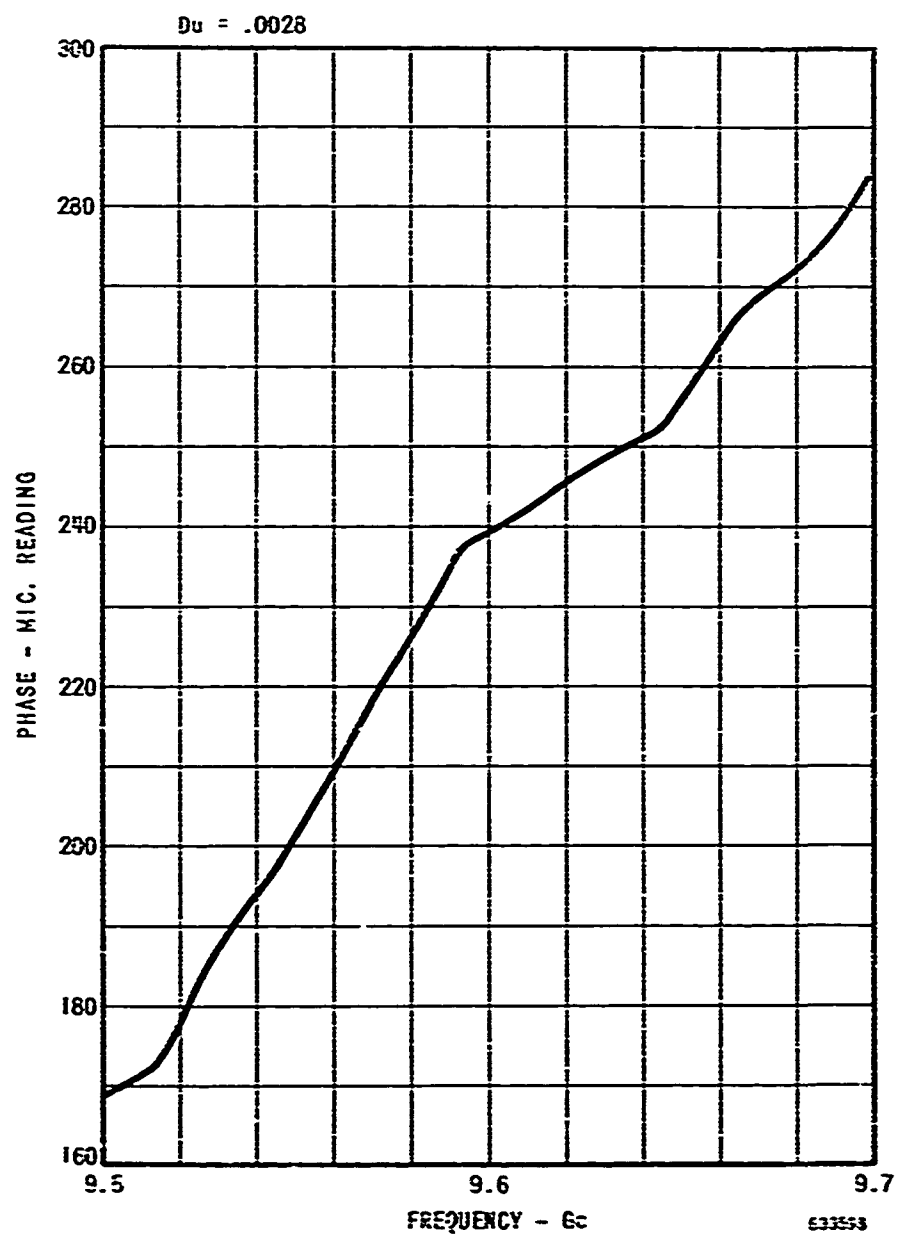
FIGURE 39   PHASE vs FREQUENCY   QKS1243/1244   CHAIN #4
(uncorrected)
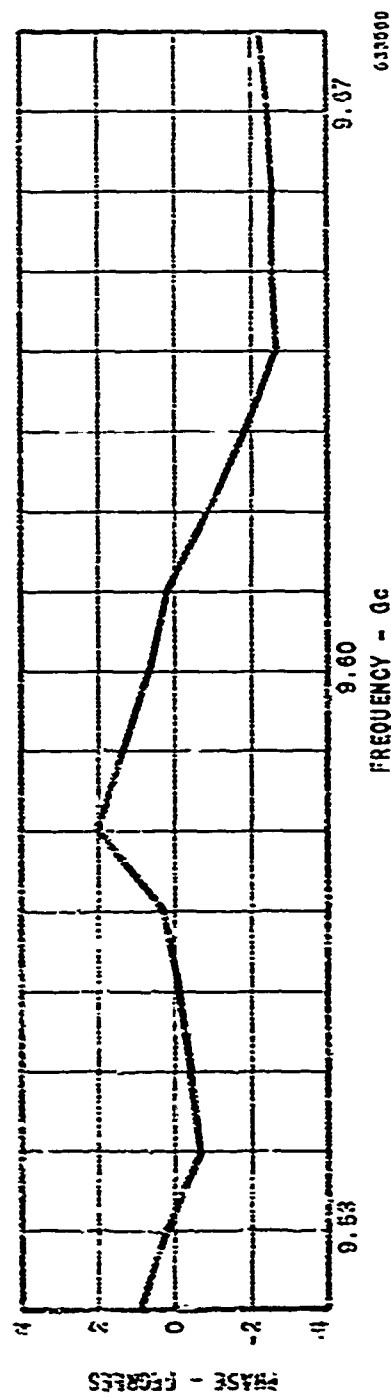
PHASE LOOP CORRECTION CURVE
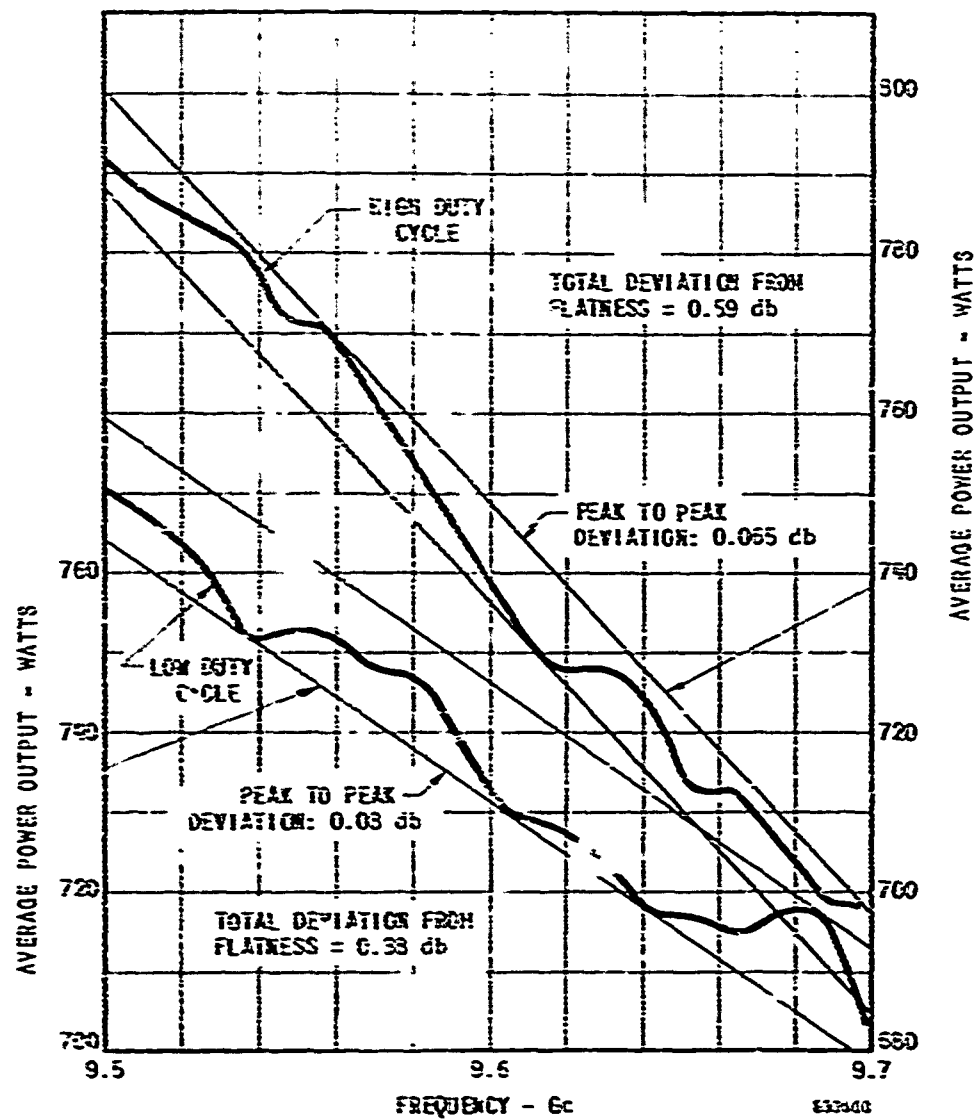
FIGURE 40

AVERAGE POWER OUTPUT vs FREQUENCY
QKS1243/1244 AMPLIFIER CHAIN #3
(EXPANDED SCALE)

73
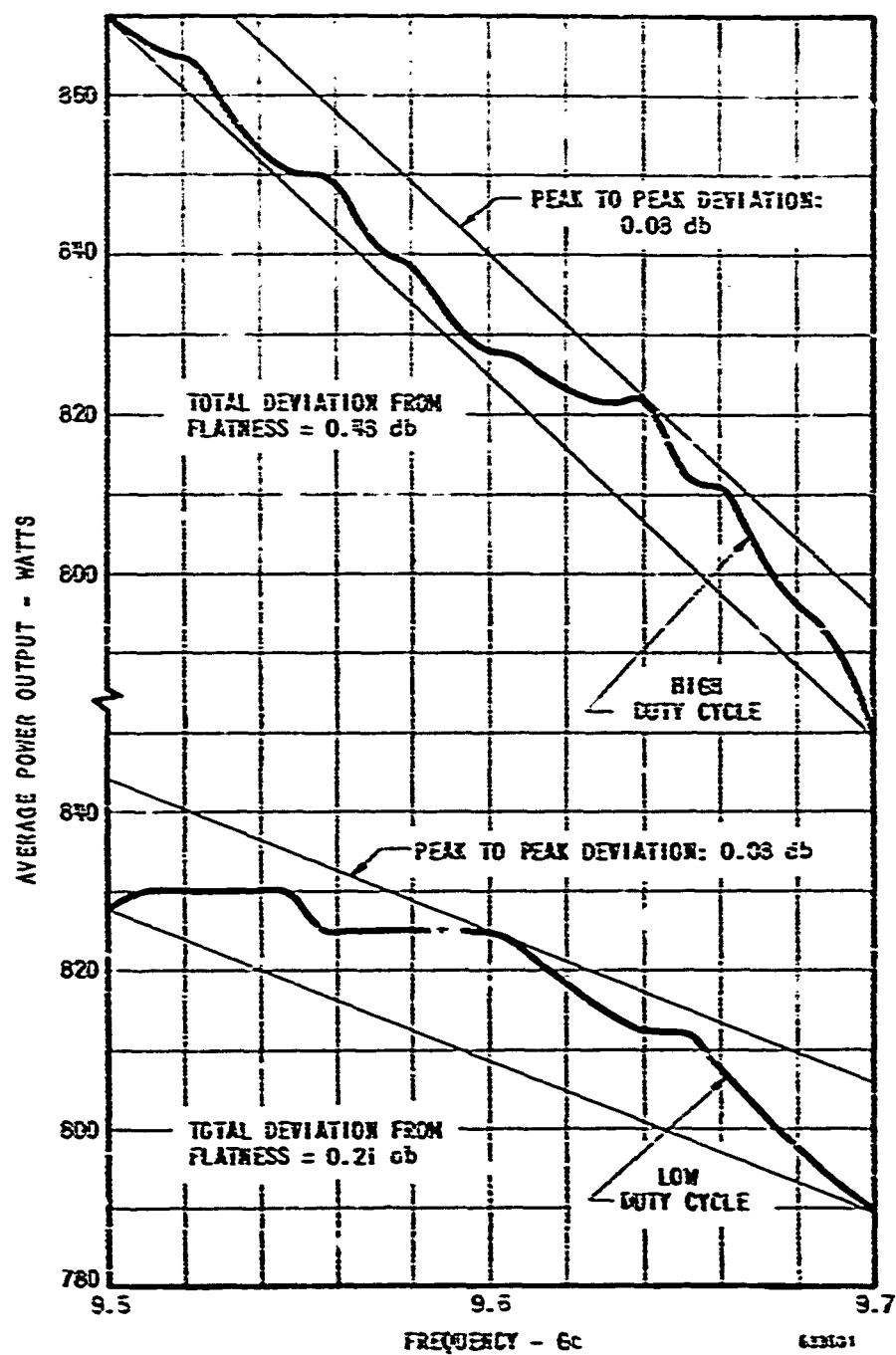
FIGURE 42   AVERAGE POWER OUTPUT vs FREQUENCY
GXS1243/1244 AMPLIFIER CHAIN #4
(EXPANDED SCALE)

- 74 -

5.4.8 Consideration of the Effect of Linear Amplitude Variation

5.4.8.1 Goldman[7] has analyzed, using paired echo theory, the low pass case of a network having an amplitude function $A(\omega) = \frac{a_0}{2} + a_1 \cos c \omega$. By extending his analysis to the bandpass case we need not restrict ourselves to the conditions of an even amplitude function and an odd phase function. We are then free to investigate the interesting case for which.

$$A(\omega) = \frac{a_0}{2} + a_1 \sin c \omega$$

(1)

$$B(\omega) = -b_0 \omega$$

where $\omega = (\omega' - \omega_0) = 2\pi (f - f_0)$
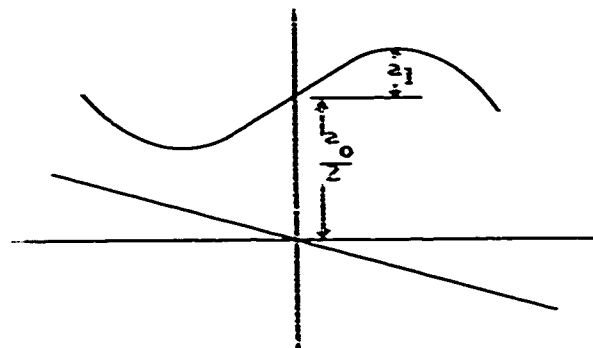
The response $\bar{G}(t)$ of a network having the amplitude and phase functions (1) to a real input expressed as $R_e \left\{ G(t) \epsilon^{j\omega t} \right\}$ is found as follows

---

7 loc cit

(2) $\overline{G}(t) = \frac{1}{2\pi} \int_{-\infty}^{\infty} S(\omega) \left(\frac{a_0}{2} + a_1 \sin c\omega \right) \epsilon^{j\left[\omega t - b_0\omega + \phi_{(\omega)} \right]} d\omega$

(3) $\overline{G}(t) = \frac{1}{2\pi} \int_{-\infty}^{\infty} S(\omega) \left(\frac{a_0}{2} + \frac{a_1}{2j} \epsilon^{jc\omega} - \frac{a_1}{2j} \epsilon^{-jc\omega} \right) \epsilon^{j\left[\omega t - b_0\omega + \phi_{(\omega)} \right]} d\omega$

(4) $\overline{G}(t) = \frac{a_0}{2} \cdot \frac{1}{2\pi} \int_{-\infty}^{\infty} S(\omega) \epsilon^{j\left[\omega(t-b_0) + \phi_{(\omega)} \right]} d\omega + \frac{a_1}{2j} \cdot \frac{1}{2\pi} \int_{-\infty}^{\infty} S(\omega) \epsilon^{j\left[\omega(t-b_0 + c) + \phi_{(\omega)} \right]} d\omega$

$\qquad\qquad - \frac{a_1}{2j} \cdot \frac{1}{2\pi} \int_{-\infty}^{\infty} S(\omega) \epsilon^{j\left[\omega(t - b_0 - c) + \phi_{(\omega)} \right]} d\omega$

(5) $\overline{G}(t) = \frac{a_0}{2} G(t-b_0) + j \left[\frac{a_1}{2} G(t - b_0 + c) - \frac{a_1}{2} G(t - b_0 - c) \right]$

The real output is then

(6) $\qquad R_e \left\{ \overline{G}(t) \epsilon^{j\omega t} \right\} = \overline{G}_I(t) \cos \omega t - \overline{G}_Q(t) \sin \omega t$

and thus the amplitude of the response is $\left| \overline{G}(t) \right|$

(7) $\overline{G}(t) = \frac{a_0}{2} G_I - \frac{a_1}{2} G_{Q+} + \frac{a_1}{2} G_{Q-} + j \left[\frac{a_0}{2} G_Q + \frac{a_1}{2} G_{Q+} - \frac{a_1}{2} G_{Q-} \right]$

where G_I and G_Q refer to the in phase and quadrature components

therefore

$$(8) \left| \bar{G}(t) \right|^2 = \left[\frac{a_0}{2} G_I(t - b_0) - \frac{a_1}{2} G_Q(t - b_0 + c) + \frac{a_1}{2} G_Q(t - b_0 - c) \right]^2$$

$$+ \left[\frac{a_0}{2} G_Q(t - b_0) + \frac{a_1}{2} G_I(t - b_0 + c) - \frac{a_1}{2} G_I(t - b_0 - c) \right]^2$$

We now approximate the actual linear power variation by a portion of a sine curve. This approximation occurs as c becomes very small and a_1 grows. In the limit the paired echos of (8) will cancel due to their opposing polarities and the output will be distortion free. We conclude therefore that the presence of a moderate linear variation of pulse amplitude may be neglected.

5 4 8 2   Following the above analysis, but assuming a cosine (even) amplitude variation on the pulse, the result becomes

$$(9) \left| \bar{G}(t) \right|^2 = \left[\frac{a_0}{2} G_I(t - b_0) + \frac{a_1}{2} G_I(t - b_0 + c) + \frac{a_1}{2} G_I(t - b_0 - c) \right]^2$$

$$+ \left[\frac{a_0}{2} G_Q(t - b_0) + \frac{a_1}{2} G_Q(t - b_0 + c) + \frac{a_1}{2} G_Q(t - b_0 - c) \right]^2$$

This is a case which would be of interest when examining the behavior of a device exhibiting a 1 or 3 db bandwidth across the pulse such as a klystron amplifier. Here however, because of the like polarities the paired echos will always add.

5 4 8 3   In the measured test data of Figures 41 and 42 the worst amplitude deviation from linearity was ± 0.04 db. This deviation of itself will result in a time sidelobe level of only -52.8 db

6 0   CONCLUSION AND RECOMMENDATIONS

6 1   The QKS1243/1244 program was successfully concluded by the delivery of three amplifier chains after demonstration of complete compliance with the specifications   These chains are expected to provide most satisfactory service in a high resolution radar system

6.2   On future procurements, the following improvements are recommended

(a)   The QKS1243 Amplitron weight can be reduced by as much as 5 lb. and its form factor can be improved with respect to vibration requirements by utilizing a new magnet design similar to that of the KS1244

(b)   Some minor changes of the QKS1243 cooling fin geometry will provide an improved product   The addition of a few cooling fins and the use of larger inter-fingaps is recommended.

(c)   Minor revisions of the QKS1244 interaction space design can result in improved efficiency in that stage to 50%.

(d)   Replacement of the present choke-type waveguide flanges with cover flange would provide cost reduction in additional tubes.

(e)   In the event that quantity deliveries of chains are anticipated the setting up of, and providing of a production line capability for these tube types should be considered.

7 0   IDENTIFICATION OF KEY TECHNICAL PERSONNEL

7 1   The QKS1243/1244 engineering program was under the general
direction of Dr. H. Scharfman, Manager of Engineering for the Microwave and
Power Tube Division and Mr. J. Skowron, Manager of the Crossed-Field Amplifier
Group   Mr. W. A. Smith, Engineering Section Head, was responsible for specific
conduct of the program.   Assisting in the tube development was Mr. R. Manchester
Mr. D Fairbank of the Mechanical and Electrical Consulting Section. Quality
Assurance Department of the Raytheon Wayland Laboratory provided cooling
analyses.

APPENDIX I

OPERATING INSTRUCTIONS - QKS1243/1244 AMPLIFIER CHAIN
AND
TEST DATA - CHAINS #2, #3, #4

- i -

RAYTHEON

OPERATING INSTRUCTIONS

QKS1243/44 AMPLIFIER CHAIN

GENERAL DESCRIPTION

The QKS1243/44 amplifier chain is comprised of two Amplitron* tubes separated by a ferrite isolator. It will produce a peak power output of 500 kilowatts when an rf drive power not less than one kilowatt is applied to its input and it will cover the frequency band 9.525 to 9.675 Gc without mechanical or electrical adjustment. Forced air cooling is utilized. The waveguide flanges of both Amplitron tubes are designed to mate with UG-51/U cover flanges and the waveguide flanges of the ferrite isolator are designed to mate with UG-52A/U choke flanges having their tapped holes drilled for clearance.

INSTALLATION AND HANDLING

The tubes should be handled by their magnets and not the input or output waveguides. When first unpacked the tubes and isolator should be examined for possible mechanical defects which may have developed during shipment. Extreme care should be exercised in installing the tubes in the equipment, for, although a tube's appearance may create the impression of great structural strength, many of the internal components are delicate. The use of non-magnetic bolts, nuts, washers and tools will be required during installation. Each tube should be mounted so that its cathode axis is normally vertical.

Cooling of the tubes will require suitable ductwork to confine the air circulation and blowers equivalent to the following:

For the QKS1244: AXIMAX-3 High slip vaneaxial fan with motor #387JS(3Ø,400cps,200 volts) Mfr.: Rotron

For the QKS1243: AVAX-4.5-1C, part #19A-894 High slip vaneaxial fan (3Ø,400cps, 200 volts) Mfr.: Globe Industries

The positive pulse voltage connection is made to the body of each tube which should be grounded. In the case of the QKS1243 Amplitron, negative voltage is applied to the high voltage binding post at the extremity of the ceramic input bushing. In the case of the QKS1244 Amplitron the binding post directly on the axis of the ceramic input bushing is the common heater-cathode connector and the binding post located off the axis of the bushing is the cathode connector. Care should be taken in affixing leads to the tubes to avoid excessive torque.

*Trademark of Raytheon Company

RAYTHEON COMPANY

RAYTHEON

ISOLATION

It is strongly urged that suitable ferrite isolation be provided between the amplifier chain and the TWT driver. Output isolation will not be required if the load VSWR is less than 1.3.

TUBE OPERATION.

When first set up, before applying heater power or high voltage to the tubes, rf drive power should be applied and it will pass through the tubes suffering only a small loss. If, as a result of some mishap, the vacuum within the tube has become lost, the rf drive power will be absorbed within the tube and negligible rf feed-through will be obtained. Under such circumstances, no heater or high voltage should be applied.

Preheat AC power may then be applied to the QKS1244 Amplitron as follows: $E_f = 1.6$ volts – $I_f = 6.3$ amps. A 3-minute warmup time is advised. Following the pre-heat cycle, providing the cooling system is operating, high voltage may be applied. It is recommended that this be done sequentially, at least until familiarity with the tubes has been obtained, by switching on first the QKS1244 and checking for proper operating before proceeding. Failure to obtain stable operation can mean either of two things:

(a) applied voltage is too high

(b) voltage is being applied prior to the rf drive pulse (trigger misalignment)

When stable operation of the QKS1244 has been obtained, the QKS1243 may be turned on. Snap on of both tubes is permissible provided that it immediately results in stable performance—if it does not, the most likely cause of instability is either (a) or (b) above. Operation of a tube in such a condition can cause irreparable damage to the cathode. Thus, under no conditions should the tubes be operated in the absence of rf drive power. The rf drive pulse should overlap the Amplitron modulating pulse to provide rf drive before and throughout the Amplitron pulse. The amount of overlap is optional.

PULSE CONDITIONS

Pulse conditions are given in the attached test data. Operation under other pulse conditions can result in damage to the Amplitron if the deviation from the given conditions is large.

PRESSURIZATION (AIR)

The input bushing should be pressurized to 14 psia minimum. The output waveguide should be pressurized to 25 psia minimum. The interstage and input waveguide runs should be pressurized to 14 psia minimum.

VIBRATION

The QKS1243/44 amplifier chain, when properly mounted will withstand the vibration conditions specified for Class I equipment by MIL-E-5400. Proper mounting includes firm support of all waveguide flanges, the isolator, the QKS1244 with 4 bolts and the QKS1243 with 2 bolts and 2 brackets, the latter providing support in a plane perpendicular to the plane of the bolts. Raytheon will provide detailed mounting recommendations upon request.

PROTECTION

The following guidelines are suggested.

(1) Interlock to prevent application of high voltage in the absence of forced air cooling.

(2) Control circuitry to prevent the application of high voltage in the absence of adequate rf drive.

(3) Spark gap to prevent input bushing breakdown in the event of overvoltage.

(4) Interlocks to prevent tube operation in the absence of proper pressurization.

QKS1243/1244 AMPLIFIER CHAIN

GENERAL INFORMATION

Weights:

QKS1243	35.0 pounds
QKS1244	8.5 pounds
IXH 24	2.1 pounds

Anode-Cathode Capacitance

QKS1243	13.6 $\mu\mu$f
QKS1244	18.4 $\mu\mu$f

TEST DATA - QKS1243/1244 CHAIN #2

August 21, 1964

Freq. Mc	Avg. Power Watts	Phase Mic. Rdg	Phase Sensitivity Degrees/1% Δi	Voltage kV	Current mA
9501	771	194		15.87 35.80	8.25-1244 39.39-1243
9513	760	214.5			
9524	743	227.5			
9536	730	243.5			
9547	722	254.0			
9558	730	264.9			
9570	735	262 5			
9581	744	265 5			
9593	754	265.8			
9604	760	266.0	0.55° - QKS1243 0.04° - QKS1244		
9616	770	267.5			
9628	780	27.3			
9640	780	276.5			
9652	780	282.5			
9664	789	285.9			
9675	796	285.9			
9687	802	283.0			
9699	804	284.5		16.35 37.10	8.0 - 1244 38.0 - 1243

Conditions

$pri = 700$ pps

QKS1243 - t_p = 2.0 μs

QKS1244 - t_p = 2.2 μs

TEST DATA - QKS1243/1244 CHAIN #2
August 21, 1964

Freq. Mc	Avg. Power Watts	Phase Mic. Rdg	Phase Sensitivity Degrees/1% Δi	Voltage kV	Current mA
9501	868	305.3		{15.9	16.65-1244
				{34.7	45.2 -1243
9513	845	322.5			
9524	814	329.5	{0.34° - QKS1243		
			{0.72° - QKS1244		
9536	781	342			
9547	772	352			
9558	755	355			
9570	755	359			
9581	765	361			
9593	768	362			
9604	773	364	{0.58° - QKS1243		
9616	781	368			
9628	785	366			
9640	781	370			
9652	786	376			
9664	790	380			
9675	793	381	{0.47° - QKS1243		
			{0.90° - QKS1244		
9687	789	366			
9699	785	391.5		{16.2	15.9-1244
				{35.6	41.8-1243

Conditions

prf = 1400 pps

QKS1243 t_p = 2.0 µs

QKS1244 t_p = 2.2 µs

TEST DATA QKS1243/1244 CHAIN #3

Freq. Mc	Avg. Power Watts	Phase Mic. Rdg	Phase Sensitivity Degrees/1% Δi	Voltage kV	Current mA
9501	770	821		$\begin{cases} 16.15 \\ 37.1 \end{cases}$	7.1 for 1244 36.5 for 1243
9513	766	825			
9524	762	826.5	$\begin{cases} 0.19^\circ \text{ (QKS1244)} \\ 0.615^\circ \text{(QKS1243)} \end{cases}$		
9536	752	828.5			
9547	752	835.5			
9558	752	835.5			
9570	748	835.5			
9581	746	834			
9593	738	839			
9504	730	846	$\begin{cases} 0.39^\circ \text{(QKS1244)} \\ 0.48^\circ \text{(QKS1}\cdots\text{)} \end{cases}$		
9616	728	849.5			
9628	724	849.5			
9640	717	846.5			
9652	717	846			
9664	715	844			
9675	717	841	$\begin{cases} 0.18^\circ \text{ (QKS1244)} \\ 0.56^\circ \text{ (QKS1243)} \end{cases}$		
9687	717	842			
9699	704	847		$\begin{cases} 16.56 \\ 37.7 \end{cases}$	7.0 for 1244 36.0 for 1243

Conditions

$prf = 700$ pps

QKS1243 $t_p = 2.0$ μs

QKS1244 $t_p = 2.2$ μs

TEST DATA QKS1243/1244 CHAIN #3

Freq. Mc	Avg. Power Watts	Phase Mic. Rdg	Phase Sensitivity Degrees/1% Δi	Voltage kV	Current mA
9501	791	883	$\{$ 0. 18° (QKS1244) $\{$ 0. 435°(QKS1243)	$\{$ 16. 31 $\{$ 36. 0	12. 5 for 1244 44. 2 for 1243
9513	787	887			
9524	784	889. 5			
9536	780	894. 5			
9547	772	899			
9558	770	904			
9570	761	907			
9581	753	909. 5			
9593	744	912. 5			
9604	736	917	$\{$ 0. 26° (QKS1244) $\{$ 0. 72° (QKS1243)		
9616	728	917. 5			
9628	728	916			
9640	725	913. 5			
9652	713	915			
9664	712	918. 5			
9675	706	915. 5			
9687	698	917			
9699	699	916. 5	$\{$ 0. 22° (QKS1244) $\{$ 0. 695°(QKS1243)	$\{$ 16. 65 $\{$ 36. 6	12. 0 for 1244 43. 0 for 1243

Conditions

prf = 1400 pps

QKS1243 t_p = 2. 0 μs

QKS1244 t_p = 2. 2 μs

TEST DATA QKS1243/1244 CHAIN #4

Freq. Mc	Avg. Power Watts	Phase Mic. Rdg.	Phase Sensitivity Degrees/1% Δi		Voltage kV	Current mA
9501	828	817	0.595° (QKS1244)	1.27° (QKS1243)	16.03 36.7	7.5 for 1244 37.5 for 1243
9513	830	825				
9524	830	831	0.53° (QKS1244)	1.0° (QKS1243)		
9536	830	834				
9547	830	841	0.545° (QKS1244)	0.99° (QKS1243)		
9558	825	846				
9570	825	854				
9581	825	860				
9593	825	864				
9604	825	873	0.42° (QKS1244)	0.81° (QKS1243)		
9616	820	874				
9628	816	874				
9640	812	873				
9652	812	879				
9664	805	885				
9675	800	889				
9687	794	892				
9699	790	895	0.35° (QKS1244)	0.71° (QKS1243)	16.35 37.3	7.0 for 1244 36.0 for 1243

Conditions

prf = 700 pps

QKS1243 t_p = 2.0 μs

QKS1244 t_p = 2.2 μs

TEST DATA QKS1243/1244 CHAIN #4

Freq. Mc	Avg. Power Watts	Phase Mic Rdg.	Phase Sensitivity Degrees/1%∆i		Voltage kV	Current mA
9501	870	169	0.51° (QKS1244) 0.50° (QKS1243)	15.87 35.7		12.5 for 1244 44.6 for 1243
9513	866	172				
9524	864	182				
9536	855	192				
9547	851	199				
9588	850	208				
9570	841	218				
9581	838	226				
9593	830	237.5				
9604	828	240	0.33° (QKS1244) 1.05° (QKS1243)			
9616	825	244				
9626	822	248				
9640	822	251				
9652	812	257				
9644	810	266				
9675	799	270				
9687	793	275				
9699	780	284	0.35° (QKS1244) 0.415° (QKS1243)	16.23 36.4		12.0 for 1244 42.0 for 1243

Conditions

$$prf = 1400 \text{ pps}$$
$$QKS1243 \; t_p = 2.0 \; \mu s$$
$$QKS1244 \; t_p = 2.2 \; \mu s$$

DISTRIBUTION LIST

Contract DA36-039-AMC-03202(E)	No. of Copies
OASD (R and E) Attn: Technical Library Room 3B1065, The Pentagon Washington, D.C. 20301	1
Commander Defense Documentation Center Attn: TISIA Cameron Station, Bldg. 5 Alexandria, Virginia 22514	20
Advisory Group on Electron Devices 346 Broadway 8th Floor New York, New York 10013	3
Director U.S. Naval Research Laboratory Attn: Code 2027 Washington, D.C. 20390	1
Commanding Officer and Director U.S. Navy Electronics Laboratory San Diego 52, California Attn: Library	1
Chief Bureau of Ships Department of the Navy Attn: 681A-1 Washington 25, D.C.	1
Systems Engineering Group Deputy for Systems Engineering Directorate of Technical Publications and Specifications (SEPRR) Wright-Patterson AFB, Ohio 45433	1

Commander, AF Cambridge Research Laboratories
Attn: CCRR (1 cy)
     CCSD (1 cy)
     CRZC (1 cy)
L. G. Hanscom Field
Bedford, Massachusetts
	3

Commander, AF Cambridge Research Laboratories Attn: CRXL-R, Research Library L. G. Hanscom Field Bedford, Massachusetts	2

Contract DA-36-039-AMC-03202(E)	No. of Copies
AFSC Scientific/Technical Liaison Office U. S. Naval Air Development Center Johnsville, Pennsylvania 18974	1
Chief, U.S. Army Security Agency Attn: AC of S, G4 (Tech Library) Arlington Hall Station Arlington 12, Virginia	2
Chief of Research and Development OCS Department of the Army Washington 25, D.C.	2
Deputy President U.S. Army Security Agency Board Arlington Hall Station Arlington 12, Virginia	1
Commanding Officer Harry Diamond Laboratories Connecticut Avenue and Van Ness Street, N. W. Washington, D.C. 20438 Attn: Library, Rm. 211, Bldg. 92	1
Commander U.S. Army Missile Command Attn: Technical Library Redstone Arsenal, Alabama	1
Commanding Officer U.S. Army Electronics Materiel Support Agency Attn: SELMS-ADJ Fort Monmouth, New Jersey 07703	1
Director USAEGIMRADA Attn: ENGGM-SS Fort Belvoir, Virginia 22060	1
Marine Corps Liaison Office U.S. Army Electronics Laboratories U.S. Army Electronics Command Attn: AMSEL-RD-LNR Fort Monmouth, New Jersey 07703	1
Director U.S. Army Electronics Laboratory U.S. Army Electronics Command Attn: Special Assistant for Research Fort Monmouth, New Jersey 07703	1

Contract DA36-039-AMC-03202(E)	No. of Copies

Director
U.S. Army Electronics Laboratories
U.S. Army Electronics Command
Attn: AMSEL-RD-PR (Contracts) (1 cy)
    AMSEL-RD-PR (Tech. Staff) (1 cy)
    AMSEL-RD-PRT (Mr. Kaplan) (1 cy)
    AMSEL-RD-PRG (Mr. Zinn) (1 cy)
Fort Monmouth, New Jersey 07703   4

Director
U.S. Army Electronics Laboratories
U.S. Army Electronics Command
Attn: Logistics Division (For: AMSEL-RD-PRM,
    Project Engineer)
Fort Monmouth, New Jersey 07703   1

Director
U.S. Army Electronics Laboratories
U.S. Army Electronics Command
Attn: Logistics Division (For: AMSEL-RD-PRM,
    Record File Copy)
Fort Monmouth, New Jersey 07703   1

Commanding General
U.S. Army Materiel Command
Attn: R and D Directorate
Washington, D.C. 20315   2

Commanding General
U.S. Army Combat Developments Command
Communications-Electronics Agency
Fort Huachuca, Arizona 85613   1

Commanding General
U.S. Army Combat Developments Command
Attn: CDCMR-E
Fort Belvoir, Virginia 22060   1

Hq., Electronics Systems Division
Attn: ESTI
L. G. Hanscom Field
Bedford, Massachusetts   1

Director, Monmouth Office
U.S. Army Combat Developments Command
Communications-Electronics Agency, Bldg. 410
Fort Monmouth, New Jersey 07703   1

AFSC Scientific/Technical Liaison Office
Attn: AMSEL-RD-LNA
Fort Monmouth, New Jersey 07703   1

Contract DA36-039-AMC-03202(E)	No. of Copies

USAEL Liaison Officer
Rome Air Development Center
Attn: RAOL
Griffiss AFB, New York 13442 1

Commander
U.S. Army Research Office (Durham)
Box CM - Duke Station
Durham, North Carolina 1

Commanding Officer
U.S. Army Engineering Research and Development
  Laboratories
Attn: STINFO Branch
Fort Belvoir, Virginia 22060 2

Director
U.S. Army Electronics Laboratories
U.S. Army Electronics Command
Attn: AMSEL-RD-ADO-RHA
Fort Monmouth, New Jersey 07703 1

Commanding Officer
U.S. Army Electronics Research and Development Activity
Attn: AMSEL-RD-WS-A
White Sands, New Mexico 88002 1

Director, Materiel Readiness Directorate
Hqs., U.S. Army Electronics Command
Attn: AMSEL-MR
Fort Monmouth, New Jersey 07703 1

Director
U.S. Army Electronics Laboratories
U.S. Army Electronics Command
Attn: Tech Documents Center (AMSEL-RD-ADT)
Fort Monmouth, New Jersey 07703 1

Director
U.S. Army Electronics Laboratories
U.S. Army Electronics Command
Attn: AMSEL-RD-P
Fort Monmouth, New Jersey 07703 1